DIELECTROPHORESIS OF INORGANIC COLLOIDAL SUSPENSIONS

By

CYNTHIA GAIL SCRIMAGER

Bachelor of Science

University of California at Berkeley

Berkeley, California

1973

Submitted to the Faculty of the Graduate College
of the Oklahoma State University
in partial fulfillment of the requirements
for the Degree of
MASTER OF SCIENCE
December, 1974

DIELECTROPHORESIS OF INORGANIC

COLLOIDAL SUSPENSIONS

Thesis Approved:

Herbert A. Pohl
Thesis Adviser

I. Dwaine Eubanks

John E. Moore

Dean of the Graduate College

ACKNOWLEDGMENTS

I wish to express my appreciation to Dr. Herbert A. Pohl, Research Adviser, and to thesis committee members Dr. T. E. Moore and Dr. I. D. Eubanks for their interest, time, and assistance.

TABLE OF CONTENTS

LIST OF FIGURES

Figure Page

CHAPTER I

INTRODUCTION AND THEORY

Introduction

The investigation of the dielectric behaviour of disperse systems has assumed increasing importance in the realm of colloid chemistry. The unusually large dielectric constants observed for colloids in aqueous electrolyte solutions, as well as the dielectric dispersions occurring over wide frequency ranges, reflect both volume and surface properties of the colloidal particle. An interpretation of the results of dielectric studies in terms of physical mechanisms must necessarily concern itself with the treatment of these properties.

The technique of dielectrophoresis provides an effective means by which the polarizability of heterogeneous systems may be investigated. It is the purpose of this thesis to report the application of dielectrophoresis to inorganic colloidal suspensions and to discuss its potential in the determination of appropriate mechanisms.

Theory

Numerous physical processes have been suggested as those responsible for the polarizability of disperse systems. Those to be considered here include:

(1) Maxwell-Wagner or interfacial polarization.

(2) Modified interfacial polarization.

(3) Tangential migration of the tightly-bound counterions of the surface double layer.

(4) Distortion of the diffuse portion of the double layer.

For each of the mechanisms to be discussed, two quantities are of particular importance: the relaxation time τ, which provides an indication of the frequency range in which the mechanism is operative, and the dielectric increment $\Delta\varepsilon$, a measure of the increased dielectric constant of the suspension over that of the suspending medium.

The well-known Maxwell-Wagner polarization mechanism (1) is a consequence of the differing conductivities and dielectric constants of the colloidal particle and the suspending medium and may occur in any heterogeneous system. If a step-function field is applied to the two-phase system of Figure 1 at time t=0, the electric displacements must be equal:

$$D_1 = D_2 \qquad E_1\varepsilon_1 = E_2\varepsilon_2 \tag{1}$$

where D_1, D_2 = electric displacements

ε_1 = dielectric constant of region I

ε_2 = dielectric constant of region II

As $t \to \infty$ Kirchoff's current continuity equations apply and

$$J_1 = J_2 \quad \text{or} \quad E_1\sigma_2 = E_2\sigma_2 \tag{2}$$

where σ_1 and σ_2 are the conductivities of the first and second regions, respectively. Thus, an accumulation of charge occurs at the interface as a result of the differing ease with which the charge carriers move through the two dielectric regions.

In a colloidal suspension, the charge accumulates at the particle/solution interface and appears to the external observer as an effective dipole. This leads, in turn, to an increase in the observed dielectric constant of the suspension.

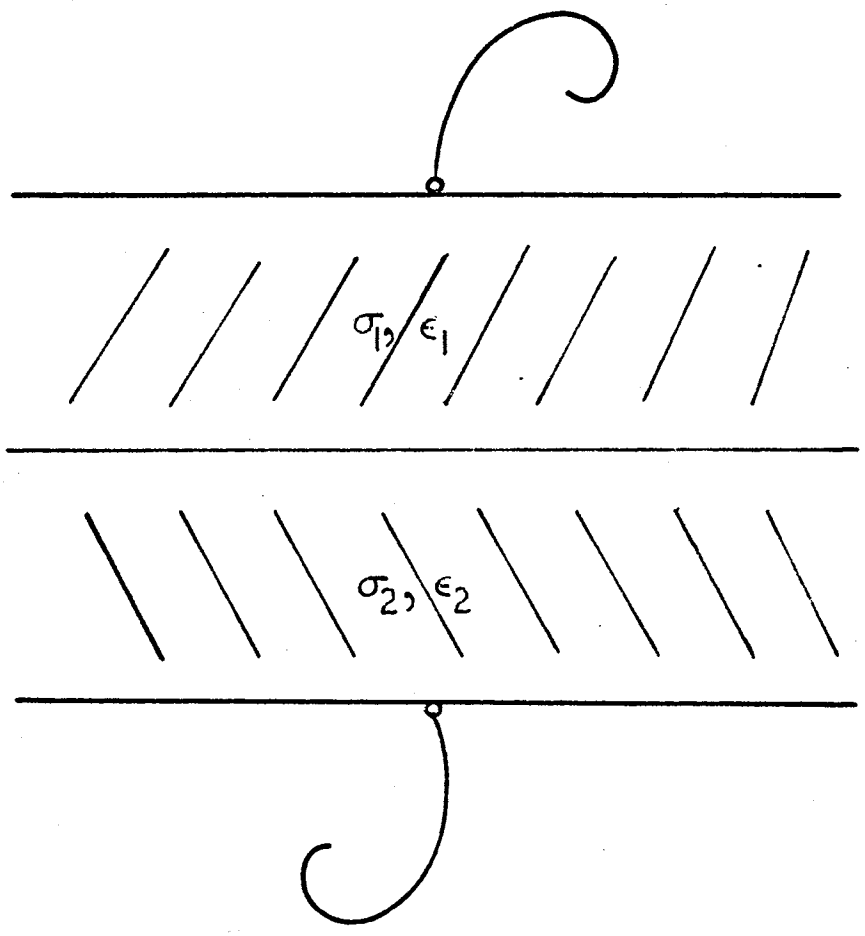

Figure 1. The Maxwell-Wagner Two-Layer Capacitor

The relaxation time for the interfacial polarization mechanism is given by (2):

$$\tau = \varepsilon_o \frac{\varepsilon_2 + 2\varepsilon_1 - p(\varepsilon_2-\varepsilon_1)}{\sigma_2 + 2\sigma_1 - p(\sigma_2-\sigma_1)} \qquad (3)$$

p = volume fraction of inclusions $\varepsilon_o = 8.85\times10^{-14}$ Coul/volt-cm

ε_1 = dielectric constant of medium

ε_2 = dielectric constant of inclusions

σ_1 = conductivity of medium

σ_2 = conductivity of inclusions

The expression for the dielectric increment of a system composed of a medium of conductivity σ_1 containing a volume fraction p of inclusions with conductivity σ_2 is:

$$\Delta\varepsilon = \frac{9p(1-p)(\varepsilon_1\sigma_2-\varepsilon_2\sigma_1)^2}{[(\varepsilon_2+2\varepsilon_1) - p(\varepsilon_2-\varepsilon_1)]\ [(\sigma_2+2\sigma_1) - p(\sigma_2-\sigma_1)]^2} \qquad (4)$$

The interfacial polarization mechanism is by definition dependent only upon the volume conductivity of the inclusions. The remaining mechanisms, on the other hand, are fundamentally concerned with the surface properties of the inclusions, in particular, with the electrical double layer.

The Electrical Double Layer

Origin of the Surface Charge

The origin of the primary surface charge of a colloidal particle must be attributed to specific interactions such as covalent bonding, van der Waal's forces or highly localized electrostatic forces. Two separate classifications of primary charge may be distinguished.

In the first, the charge is determined principally by the nature of the particle. An example is that of an oil-in-water emulsion, in which

oil droplets acquire charge by van der Waal's adsorption of hydrophobic ions such as long-chain sulfonates or sulfates. The charge acquired is essentially a constant and is independent of the constitution of the solution.

In other colloidal systems, however, the surface charge density may vary and is determined by an equilibrium between ions at the particle surface and in solution. Such ions are known as potential-determining ions and contribute significantly to the properties of the double layer. For example, the charge density of a colloidal silica particle varies with the degree of ionization of surface silanol groups according to the equation:

$$SiOH \rightarrow SiO^- + H^+ \qquad (5)$$

and is therefore highly dependent upon solution pH. It is the surface/solution equilibrium of the potential-determining hydrogen ions that is responsible for the charge of the silica surface.

The Structure of the Double Layer

A qualitative model for the structure of the electrical double layer is pictured in Figure 2a. The negatively charged surface is taken to represent the layer of ions responsible for the primary charge of the colloidal particle, with the surface charge density σ_o defined as the number of electronic charges per unit area. Immediately adjacent to the surface is a monolayer of oriented water dipoles.

The inner Helmholtz plane is the locus of desolvated, contact adsorbed ions. Contact adsorption, like the adsorption leading to the primary charge, is assumed to be non-Coulombic in nature and to arise from covalent bonding, dispersion forces or electrical image forces.

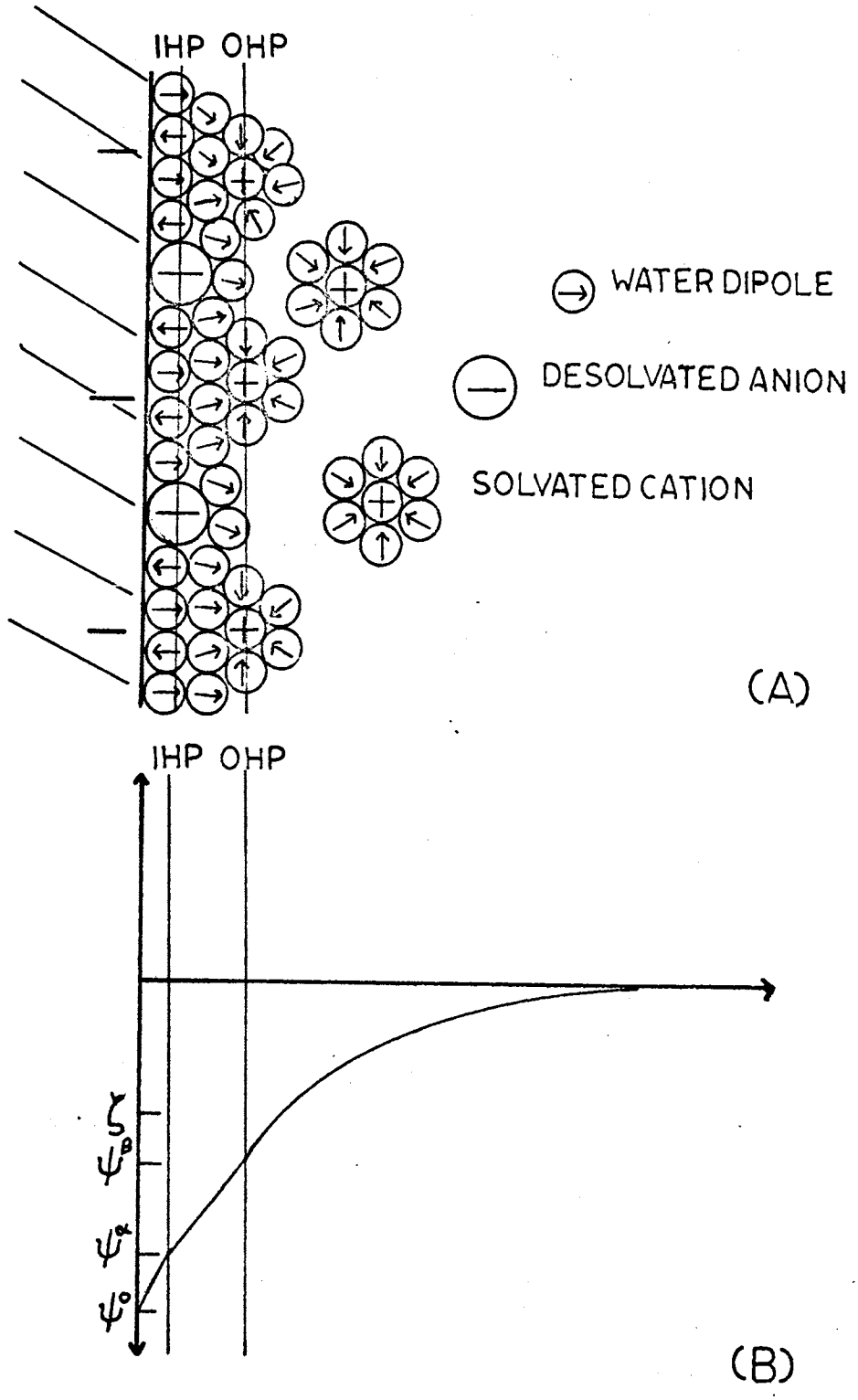

Figure 2. The Double-Layer and Associated Potentials

The sign of the free energy change associated with contact adsorption is dependent upon the relative magnitudes of the contact adsorption energy and the hydration energies of the adsorbed ions. For this reason, anions and large cations are more readily contact adsorbed than are smaller cations.

The outer Helmholtz plane is the locus of solvated, positively charged counterions. These ions are attracted to the negatively charged surface by Coulombic forces sufficient to overcome the effects of thermal agitation and may be thought of as relatively tightly bound.

The diffuse region of the double layer consists of loosely bound, solvated counterions that have been subjected to the forces of thermal randomization. The equilibrium between ions located at the outer Helmholtz plane and in the diffuse region is a dynamic one, and counterions from each of these two locations are continually exchanging. The total positive charge of the compact and diffuse regions of the double layer must, of course, exactly compensate the charge of the surface.

In Figure 2b are represented the potentials corresponding to the various boundaries of the double layer:

(1) Ψ^{o} is the potential at the surface and measures the total potential drop across the double layer.

(2) Ψ^{α}, the potential at the inner Helmholtz plane.

(3) Ψ^{β}, the potential at the outer Helmholtz plane.

(4) ζ, the potential located in the diffuse region and associated with the hydrodynamic plane of shear.

It is the zeta potential that may be experimentally determined from electrokinetic measurements. The formula for the zeta potential obtained by approximating the double layer by a parallel plate capacitor is (3):

$$\zeta = \frac{4\pi\sigma_o d}{\varepsilon_o \varepsilon_1} \qquad (6)$$

It is apparent that the zeta potential is affected by changes in either the surface charge density σ_o or the double layer thickness d, and although its value may be closely related to those of the inner potentials, it does not necessarily reflect all that occurs at the particle surface.

The Effect of Electrolytes

When an electrolyte is added to a colloidal suspension, the excess counterions accumulate at the negatively charged particle surfaces, compressing the surface double layers. In addition, the innermost counterions screen those further removed, thereby decreasing the effective charge density experienced by the outer counterions. The effect of electrolytes upon the various potentials of Figure 2b may be summarized as follows (3):

(1) In the absence of potential-determining ions, the effect of an indifferent electrolyte is simply to decrease the double-layer thickness and, correspondingly, the potentials Ψ^o and ζ. The surface charge density σ_o remains constant.

(2) If potential-determining ions are present, the surface/solution equilibrium may shift in such a way as to restore the lowered surface potential to its original value. Thus, the surface charge density σ_o increases and Ψ^o remains constant. The double layer is still compressed, however, and a greater number of ions are adsorbed at the outer Helmholtz plane. Consequently, the potentials Ψ^β and ζ are lowered.

(3) In the presence of polyvalent counterions, Coulombic adsorption may lead to a decrease in the surface charge density through the formation of ion pairs. In some cases, a sign reversal of the surface charge may occur.

The effectiveness of electrolytes in the lowering of double layer potentials is given by the empirically determined Schulze-Hardy rule, which states that in the absence of specific interactions, the concentration of electrolyte required for flocculation of colloids is inversely proportional to the ionic valence. Hence, a triply-charged ion is far more effective than a singly-charged ion in the diminution of potentials because of its greater screening capability and the increased Coulombic attraction to the oppositely charged surface. For isovalent ions, ionic radius becomes the determining factor. Smaller ions may more closely approach the outer Helmholtz plane and as a result are more tightly bound than are larger ions. The familiar Hofmeister series has been found to be applicable to flocculation values for isovalent ions. Finally, an increase in concentration of the electrolyte has the same effect as an increase in the valence of the counterions.

In order to review the origin, structure and properties of the electrical double layer, it is perhaps most instructive to consider a specific example, such as that of colloidal silica. The presently accepted theory of the silica surface was advanced by Carman (4).

In the interior of the SiO_2 colloidal particle, each silicon atom is tetrahedrally bonded to four oxygen atoms. Each oxygen atom, in turn, is bonded to two silicon atoms as pictured in Figure 3a. At the surface of the particle, however, each Si atom lacks an oxygen to complete the SiO_4 tetrahedron, and each oxygen atom is bonded to only one

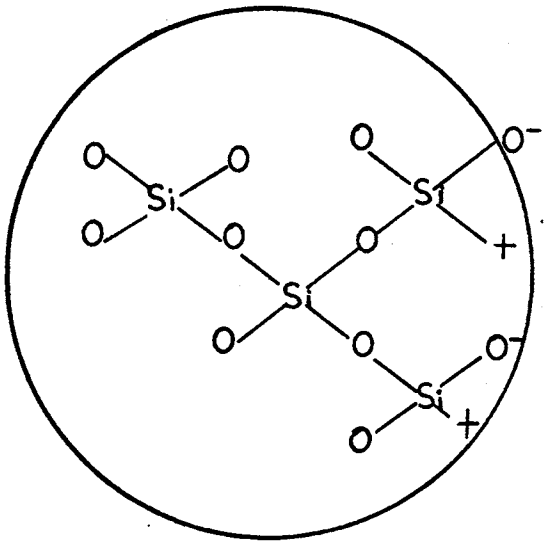

(A)

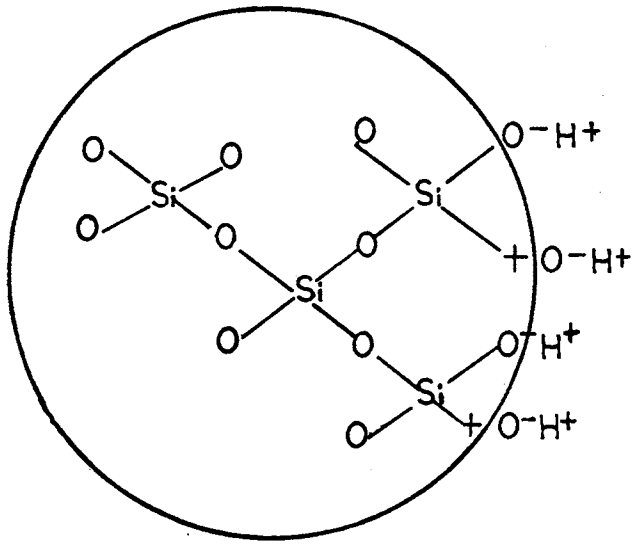

(B)

Figure 3. A Diagrammatic Representation of the SiO_2 Particle

silicon. The silicon and oxygen atoms are thus said to possess unsatisfied bonding capabilities or residual valences. In the presence of moisture, these bonding capabilities may be satisfied in the manner depicted in Figure 3b. The water molecule is regarded as an oxygen ion and two hydrogen ions. The oxygen ion completes the tetrahedron of the surface silicon, while the hydrogen ion bonds to the adjacent, negatively charged surface oxygen. This yields, in effect, "adsorbed" hydroxyl ions on the silica surface and results in the SiOH groups that may dissociate to give rise to the surface charge.

Although the precise isoelectric point (point of zero charge) of silica is not known, it is estimated to occur at a pH of around 3.5 (5); at lower values the surface silanol groups have little tendency to dissociate and instead hydrogen bond to a monolayer of water molecules. At higher pH's, the silanol groups ionize, resulting in SiO^- groups on the surface with hydrogen ions and base cations as counterions. The approximate surface charge density may be calculated from the dissociation constant for monosilicic acid (6):

$$K_a = \frac{[SiO^-]\ [H^+]}{[SiOH]} \simeq 3 \times 10^{-10} \qquad (7)$$

From structural considerations, the number of surface silanol groups has been calculated to be eight per square millimicron (7).

In a 1×10^{-6} M solution of sodium hydroxide, the silica surface is negatively charged, with hydrogen and sodium cations occupying the outer Helmholtz plane and the diffuse region. If an electrolyte such as potassium nitrate is added, potassium ions accumulate at the negatively charged particle surfaces. The double layer is compressed and the surface potential Ψ^o lowered. At this point, a number of silanol groups will dissociate in an attempt to restore the potential to its

initial value. The surface charge density will increase while the surface potential remains constant. A larger number of cations are adsorbed at the outer Helmholtz plane and into the diffuse region, however, lowering Ψ^{β} and ζ.

The addition of doubly-charged calcium ions may result in a decrease in surface charge density through the formation of ion pairs, as well as a compression of the double layer. Eventually, the double layer may completely collapse and reform with a positive surface charge.

Surface-Related Mechanisms

The electric field of the colloidal particle surface affects both the number and mobilities of ions in the double layer. It is necessary, therefore, to consider an additional region, with conductivity σ_s, in a complete development of interfacial polarization. The following treatment of modified interfacial polarization is given by O'Konski (8).

The electrical double layer is represented by a thin conducting shell surrounding the suspended particle, as shown in Figure 4. The surface conductance, $\lambda_s = \sigma_s d$, where d is the double layer thickness, may be approximated by (9):

$$\lambda_s \simeq e_o^2 \sigma_o u \qquad (8)$$

e_o = counterion charge

σ_o = surface charge density

u = mechanical mobility of counterion

The existence of the conducting shell results in the presence of another interface at which charge accumulation may occur.

To simplify the calculations, O'Konski assumes boundary conditions such that the surface conductance is included in the expression for the

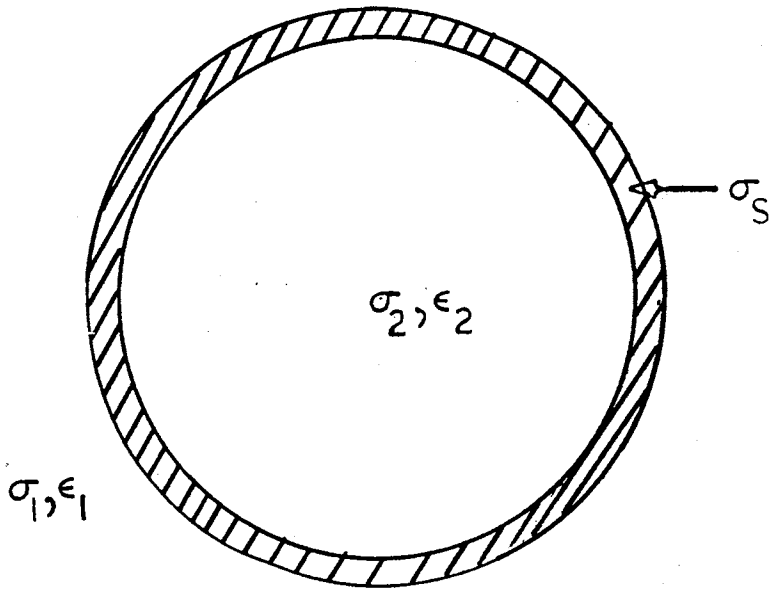

Figure 4. Particle With Thin Conducting Shell

particle volume conductivity:

$$\sigma_2' = \sigma_2 + 2\lambda_s/a \tag{9}$$

σ_2 = particle conductivity

λ_s = surface conductance

a = particle radius

The relaxation time and dielectric increment for the modified interfacial polarization mechanism are then given by (2):

$$\tau = \varepsilon_o \frac{\varepsilon_2+2\varepsilon_1-p(\varepsilon_2-\varepsilon_1)}{\sigma_2+2\lambda_s/a+2\sigma_1-p(\sigma_2+2\lambda_s/a-\sigma_1)} \tag{10}$$

$$\Delta\varepsilon = \frac{9p(1-p)(\varepsilon_2+2\varepsilon_1-p(\varepsilon_2-\varepsilon_1))}{[(\varepsilon_2+2\varepsilon_1)-p(\varepsilon_2-\varepsilon_1)]\ [(\sigma_2+\frac{2\lambda_s}{a}+2\sigma_1)-p(\sigma_2+\frac{2\lambda_s}{a}-\sigma_1)]} \tag{11}$$

It is apparent that the expressions are those for the volume interfacial polarization mechanism, with an additional term resulting from the surface conductance of the electrical double layer.

The third physical process suggested as responsible for the dielectric behaviour of disperse systems is that favored by Schwarz (10) and is pictured in Figure 5. Schwarz attributes the excess polarizability of the colloidal suspension to the redistribution of tightly-bound counterions at the outer Helmholtz plane under the influence of an applied electric field. The motion of the counterions, tangential to the partially ionized particle surface, is accomplished by thermally activated hopping from one unoccupied charged site to another. The bound counterions must overcome a potential barrier in order to move along the surface. The relaxation time for the mechanism is then dependent upon the diffusional relaxation of the counterions when the externally applied field is no longer active. This leads to the expression:

$$\tau_{\text{bound ion}} = a^2/2u_b kT \tag{12}$$

a = particle radius $\qquad$ u_b = bound ion mobility

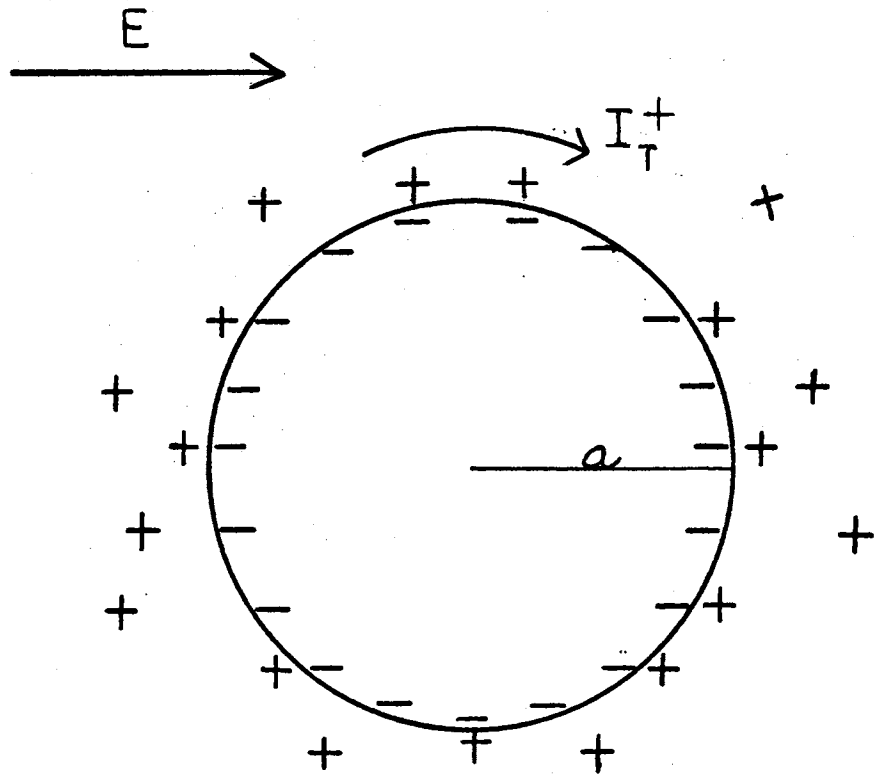

Figure 5. Illustration of Bound-Counterion Polarization--I_+^+ = Tangential Flux of Positively Charged Bound Counterions

The surface ion mobility u_b is smaller than that of free ions in solution. The two may be related by the equation:

$$u_b = u_o e^{-\alpha/kT} \tag{13}$$

where α is the height of the potential barrier and u_o is the free ion mobility. The height of the potential barrier may be approximated by:

$$\alpha \simeq \frac{e_o^2}{\varepsilon_1 \delta} \tag{14}$$

where e_o is the charge of the counterion and delta is the minimum distance between a given ion and its countercharge on the surface. For most colloids, delta is a few Angstrom units and alpha is in the order of one kilocalorie per mole. The dielectric increment is given by:

$$\Delta\varepsilon = 9/4 \; \frac{p}{(1+p/2)^2} \; \frac{e_o^2 a \sigma_o}{\varepsilon_o kT} \tag{15}$$

Schwarz's theory excludes the possibility of bound-counterion exchange with the dispersing medium and, furthermore, neglects any contribution to the particle polarizability resulting from the distortion of the diffuse portion of the double layer. The consequences of these assumptions have been thoroughly reviewed by Duhkin (11, 12).

Duhkin modifies Schwarz's expressions for the bound counterion relaxation time and dielectric increment by a factor of M^{-1},

where $$M = 1 + z^+ z^- (z^+ + z^-) \kappa \sigma_o / C_o \tag{16}$$

$z^{\pm}$ = valence of cation and anion

κ = Debye reciprocal thickness

C_o = concentration in bulk solution

The physical significance of the correction factor is illustrated in Figure 6. As the positively charged counterions move along the particle surface in response to the externally applied electric field, the local electroneutrality of the double layer is disturbed. This deviation from

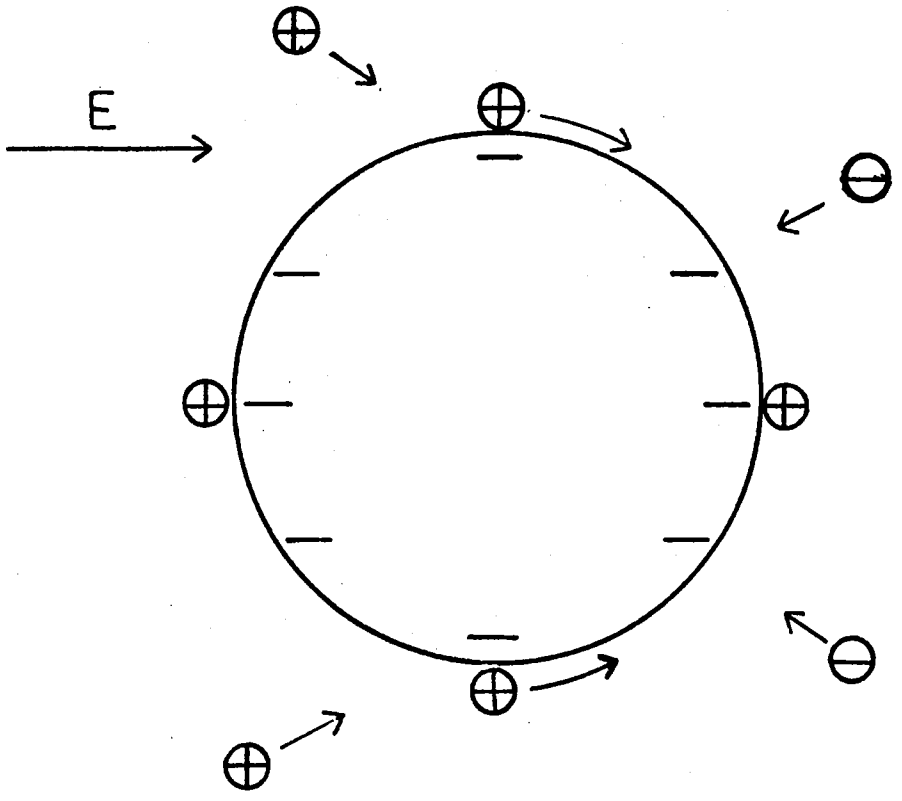

Figure 6. Illustration of the Duhkin Correction Factor

electroneutrality gives rise to a normal field component, inducing flow of ions to the surface from the solution volume. An oscillating diffuse atmosphere is established, with a polarization opposite in sign to that of the bound counterions. The magnitudes of the bound-ion relaxation time and dielectric increment are thus decreased by a factor of M^{-1}. The decrease is substantial and, according to Duhkin, illustrates the inadvisability of Schwarz's assumption.

Duhkin, in addition, considers the polarization contribution of the diffuse portion of the double layer (Figure 7). Although a continuous spread of relaxation times is possible, he conditionally assumes that:

$$\tau_{diffuse} = \frac{a^2}{2ukT} \tag{17}$$

where u is now taken to be the mechanical mobility of an essentially free counterion. The dielectric increment is given by:

$$\Delta\varepsilon \simeq 9/2\ p\ \varepsilon_1\ (3m\ \exp(e\zeta/kT) + \exp(e\Psi^{\beta}/kT))^2 \tag{18}$$

$$m = \frac{e_o^2 \varepsilon_1}{(kT)^2 6\pi\eta D}$$

ζ = zeta potential

Ψ^{β} = potential at outer Helmholtz plane

η = medium viscosity

D = counterion diffusion coefficient

In his expression for the dielectric increment, Duhkin emphasizes the previously noted distinction between the electrokinetic zeta potential and the true potential at the outer Helmholtz plane. In actual calculations, however, he equates the two and assigns an empirical value to the quantity $e\zeta/kT$ in order to secure agreement with experimental measurements.

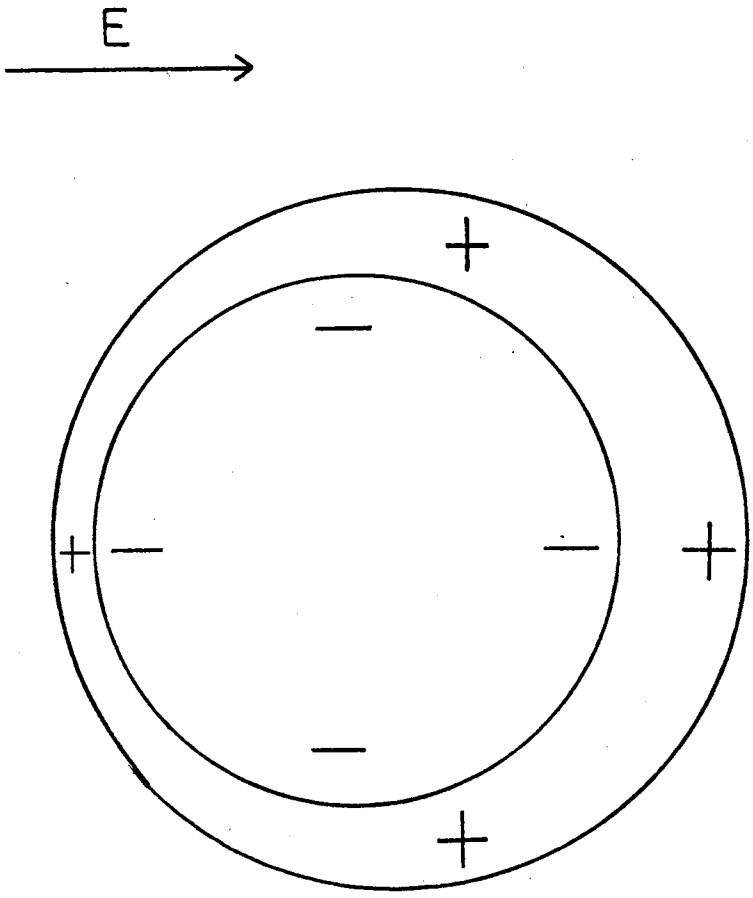

Figure 7. Illustration of Diffuse Atmosphere Polarization

Examination of the theories proposed by Schwarz and Duhkin reveals that the disparity lies principally in the assumption of double layer composition. Schwarz's treatment deals with polarization in the absence of a diffuse part of the double layer. Duhkin's theory, on the other hand, is primarily concerned with the response of the diffuse atmosphere.

The actual structure of the double layer is determined by experimental conditions. At relatively high electrolyte concentrations, a considerable number of the counterions are localized at the outer Helmholtz plane. At lower concentrations the population of the diffuse region is appreciable. (The electrolyte concentration at which the filling of the outer Helmholtz plane must be taken into account is dependent upon the association constant for the charged-site/counterion pair and therefore upon the particular type of counterion.) Under conditions of high electrolyte concentration, and if bound counterion exchange is recognized, Schwarz's expressions for the relaxation time and dielectric increment are appropriate--at low electrolyte concentrations, Duhkin's theory is applicable. A precise delineation is not possible, and at intermediate concentrations either theory may be acceptable. Of the two, Schwarz's expression for the dielectric increment is the more tractable. It should also be noted that both Schwarz and Duhkin treat the counterion atmosphere as a continuous distribution of charge, an approach quite different from the discrete binding site model of Mandel (13).

The four mechanisms just discussed are by no means the only ones that must be considered. They were chosen as representative of the essential features of the disperse system and as sufficiently

quantitative to allow comparison with experimental results. Other suggested mechanisms include Debye rotation (14), proton fluctuation (15), and the structural change of the water lattice (16).

The dielectric behaviour of disperse systems is customarily studied with alternating current bridge techniques (2). Bridge measurements may directly determine both the real and imaginary dielectric factors for colloidal suspensions. Such measurements require bridges specifically designed for the precise determination of dielectric constants and conductivities for highly conductive solutions. An alternative means by which the polarizability of heterogeneous systems may be investigated is provided by dielectrophoresis.

Dielectrophoresis

Dielectrophoresis has been defined by Pohl (17) as the translational motion of a neutral, polarizable body in a nonuniform electric field. Dielectrophoresis is contrasted with the more familiar electrophoresis in Figure 8a. In a uniform electric field such as that theoretically produced by two flat parallel plates, the charged body moves along the field lines in the appropriate direction. The effect is electrophoresis. The neutral body, subjected to a uniform electric field, is simply polarized and exhibits no translational motion. For the case of the nonuniform field of Figure 8b, a different situation is seen to exist. The charged particle moves as before along the field lines toward the negatively charged electrode. The neutral body is now not only polarized but drawn toward the region of highest field strength. The polarization of the particle is uniform, but the force experienced by the half adjacent to the stronger electric field region

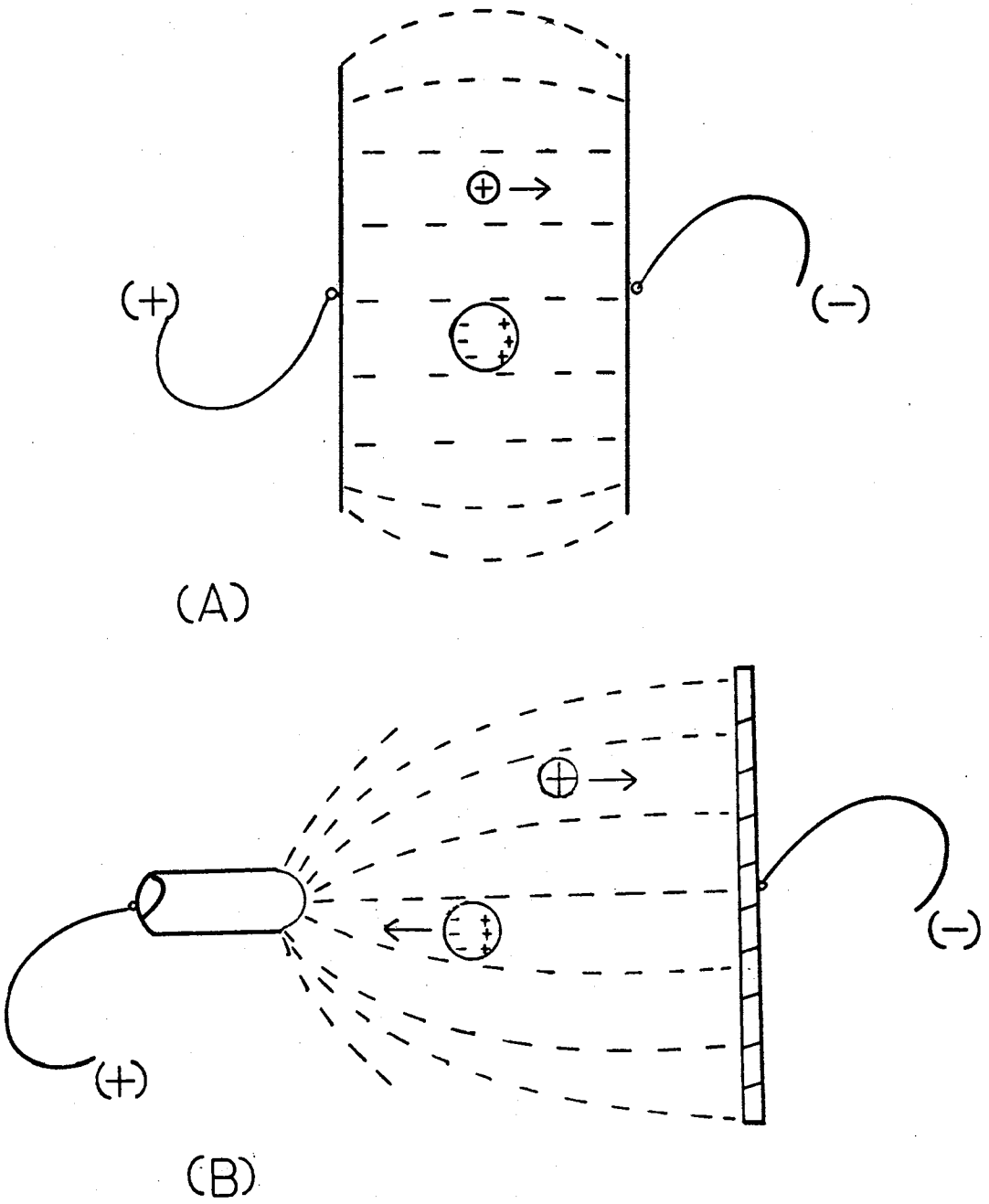

Figure 8. Illustration of Electrophoresis and Dielectrophoresis

is greater than that experienced by the remainder of the particle.

If the field is reversed, so that the electrodes change sign, the direction of motion of the charged particle is also reversed. The neutral body, however, continues to be drawn toward the high-field region. Thus, dielectrophoretic motion is independent of the sign of the electrode and dependent only upon the local electric field strength.

The expression for the dielectrophoretic force on a small, spherical, perfectly insulating particle suspended in a perfect dielectric medium is given by (18):

$$F = 2\pi a^3 K_1 \frac{K_2-K_1}{K_2+2K_1} \nabla |E|^2 \qquad (19)$$

a = particle radius

K_1 = dielectric constant of medium

K_2 = dielectric constant of particle

E = electric field intensity

Three aspects of the force should be noted:

(1) It is proportional to the cube of the particle radius.

(2) It involves the difference in the dielectric constants of particle and medium.

(3) It is dependent upon the square of the electric field intensity, allowing the use of alternating fields.

If the dielectric constant of the particle is less than that of the surrounding medium, the simple dielectrophoretic force equation predicts that the particle will experience a negative force, since the medium is more polarizable and should be preferentially attracted to the region of highest field intensity. Experimentally, it is found that if aqueous suspensions of low dielectric constant colloidal particles are subjected to non-uniform alternating electric fields, collection is appreciable

over a wide frequency range. These results indicate that the static dielectric constants of equation 19 must be replaced by complex quantities and a generalized force equation obtained (19):

$$F = 3/2\ V_2 \mathrm{Re}\ \{\varepsilon_1^* \frac{\varepsilon_2-\varepsilon_1}{\varepsilon_2+2\varepsilon_1}\}\ \nabla\ |E|^2$$

V_2 = volume of particle

ε_1^* = complex conjugate (20)

$\varepsilon_1 = \varepsilon_o K_1 - i\sigma_1/\omega \qquad \varepsilon_2 = \varepsilon_o K_2 - i\sigma_2/\omega$

The complex dielectric constants incorporate those factors, attributable to the heterogeneous nature of the system, which increase the effective polarizability of the colloidal particles.

The dielectrophoretic collection rate is proportional to the frequency-dependent effective or apparent particle polarizability. Therefore, if colloidal suspensions are subjected to non-uniform alternating fields of varying frequency, collection or yield spectra may be obtained. These spectra should exhibit collection peaks in frequency ranges corresponding to the relaxation times of contributing mechanisms. The variation of experimental conditions such as medium conductivity, solution pH, electrolyte concentration and particle size may provide further information concerning the polarization mechanisms of the disperse system.

CHAPTER II

EXPERIMENTAL METHODS

Equipment

pH

Solution pH was determined with a Beckman Zeromatic II pH meter and a Sargent-Welch S-30070-10 miniature combination electrode. The meter was standardized with pHydrion Buffer solutions (Micro Essential Laboratory).

Conductivity

Solution conductivity was measured at a frequency of 1 kHz by a General Radio 1650B impedance bridge with a resistance range of 10^{-7} ohms and an accuracy of 1 percent. A dipping-type YSI (Yellow Springs Instrument Co.) 3400 series conductivity cell with platinum-blacked electrodes was used.

Optical Density

Suspension optical density was measured by a Beckman Model B Spectrophotometer (Beckman Instruments, Inc.). No attempt was made to correlate particle concentration with suspension optical density, but the volume fractions of particles employed were determined to be less than one one-hundredth.

Microscope

Microscopic observations were made with a Bausch and Lomb Model PB-252 Dynazoom binocular microscope. Although continuous variation in magnification from 35X to 1940X was possible, all measurements were obtained at a magnification of 210X, with a 1X zoom setting, 10X eyepieces, and a 21X objective.

A 10 millimeter, 100 division reticle was mounted into one of the oculars and used to measure the dielectrophoretic yield, or linear extent of collected particles from the electrode surface. By use of an Edscorp standard graduated slide, one reticle division was found to equal 0.005 millimeters at a magnification of 210X.

Voltage Supplies

Low-frequency (5 Hz to 600 kHz) electrical excitation was supplied by a Hewlett-Packard Model 200 CD audio oscillator, providing a maximum voltage of 24 volts. Frequencies of 1, 2 and 4 MHz were supplied by an oscillator designed by Dr. Bennett L. Basore (Electrical Engineering Department, O.S.U.) in conjunction with a Heathkit Model PS-2 variable voltage regulated power supply. The voltage signal was monitored by a Hewlett-Packard Model 140A oscilloscope and the r.m.s. voltage measured by a Hewlett-Packard Model 410B vacuum tube voltmeter with an accuracy of ± 3 percent at frequencies below 400 MHz.

Procedure

Preparation of SiO_2

Ludox LS colloidal silica (Du Pont Co.) was deionized by passage through ion exchange resin and dried at 200° C. for 24 hours. The

silica powder was then ground with mortar and pestle and the desired particle size range selected by centrifugation in a Fischer Model 59 analytical centrifuge. The time required for centrifugation was calculated from the Stoke's law equation for sedimentation velocity:

$$V = \frac{2r^2(\rho-\rho^o)g}{9\eta} \qquad (21)$$

r = particle radius

ρ = density of particle

ρ^o= density of medium

g = gravitational constant

η = medium viscosity

The silica particles were then washed three times with deionized water and suspended in solutions of known pH and conductivity.

Collection Time

The quantity of interest in many-particle studies is the dielectrophoretic collection rate, or yield per unit time. The interval of time chosen for collection should ideally correspond to the point of steepest slope in the yield versus time curve. In Figure 9 are given the yield versus time curves for a number of frequencies. It may be seen that there is considerable variation in slopes and that the low-frequency collection appears to saturate after very short time intervals. From these curves, a collection time of one minute was chosen as optimum for all frequencies, although the 100 Hz collection is obviously saturated at this point.

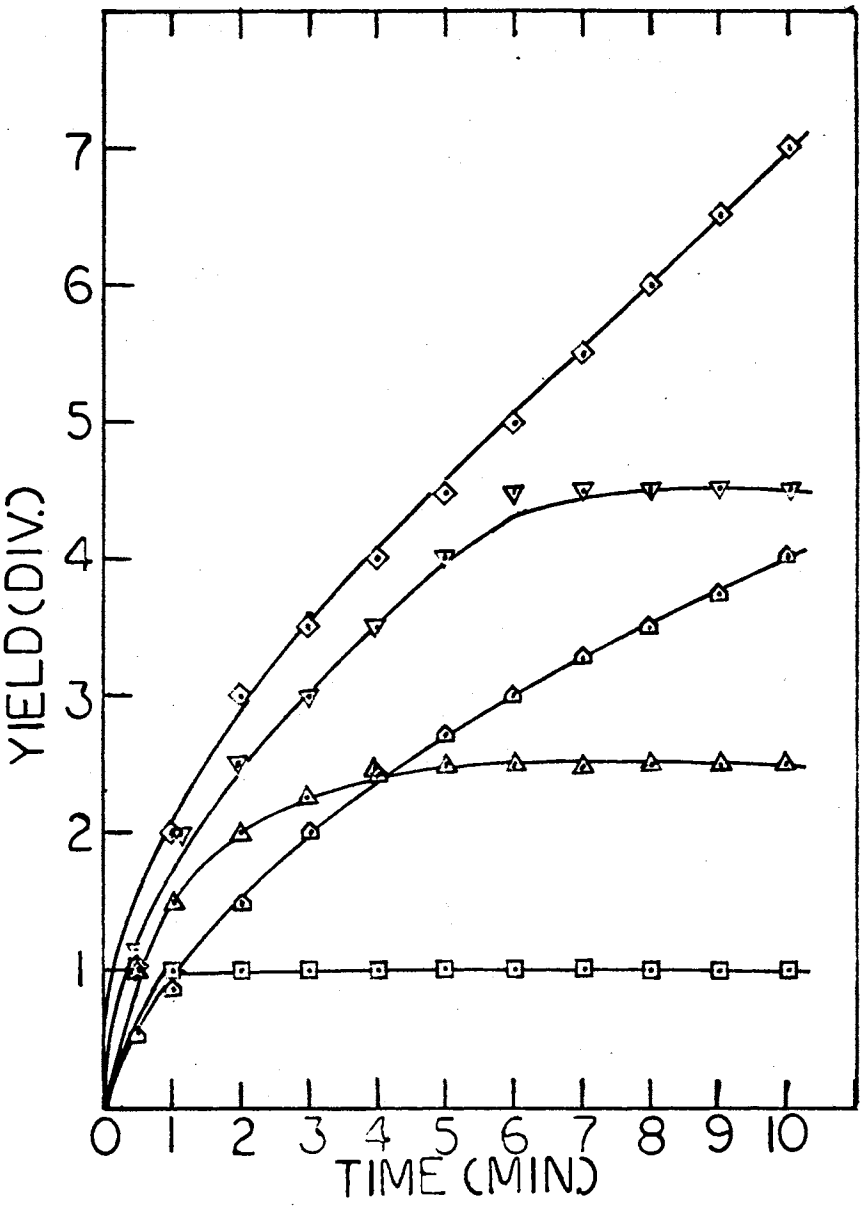

Figure 9. Yield Versus Time Curves for SiO_2; 25 Micron Diameter Wire-Wire Electrodes, 20 Volts r.m.s., Linear Flow Rate 10.2 cm/min, 210X; 0.3-0.5 Micron Particle Radius, pH=7.9, $\rho=0.37 \times 10^5$ ohm-cm, Optical Density = 0.54 at 550; (◇) = 500 kHz, (▽) = 100 kHz, (⌂) = 10 kHz, (△) = 2 kHz, (□) = 100 Hz

Cell Design

Because of the severe interelectrode circulation encountered at low frequencies, a cell design differing from those of earlier studies (20) was employed. The circulation and pulsing, probably associated with charge injection and thermal gradient effects (21, 22) were masked by a continuous flow of solution through the dielectrophoresis cell.

A diagram of the continuous cell is shown in Figure 10. Two bare platinum wires, 25 microns in diameter, were fixed to a microscope slide at a separation of around one millimeter. Perpendicular to the electrodes were placed two short lengths of 0.7 millimeter diameter Teflon tubing. A plastic coverslip was secured over the wires and the system sealed with epoxy to prevent leakage.

The solution to be studied was introduced into the tubing and cell chamber by means of a syringe mounted on a Model 975 Harvard Apparatus compact infusion pump with calibrated flow rate settings. The flow through the cell should be sufficient to overcome the interelectrode circulation, but not so rapid as to tear collected particles from the electrodes. Figure 11 shows the plot of collection versus linear flow rate (volume flow rate/chamber cross-sectional area) for some representative frequencies. From these plots, a linear flow rate of 10.1 cm./min. was chosen for all measurements. The continuous flow largely eliminated the problems of circulation and pulsing, although slight streaming of particles away from the electrode surface was still observable at very low (< 2 kHz) frequencies.

In order to obtain a collection rate versus frequency spectrum, the syringe was filled with the colloidal solution and the collection voltage and oscillator frequency selected. The solution was then passed

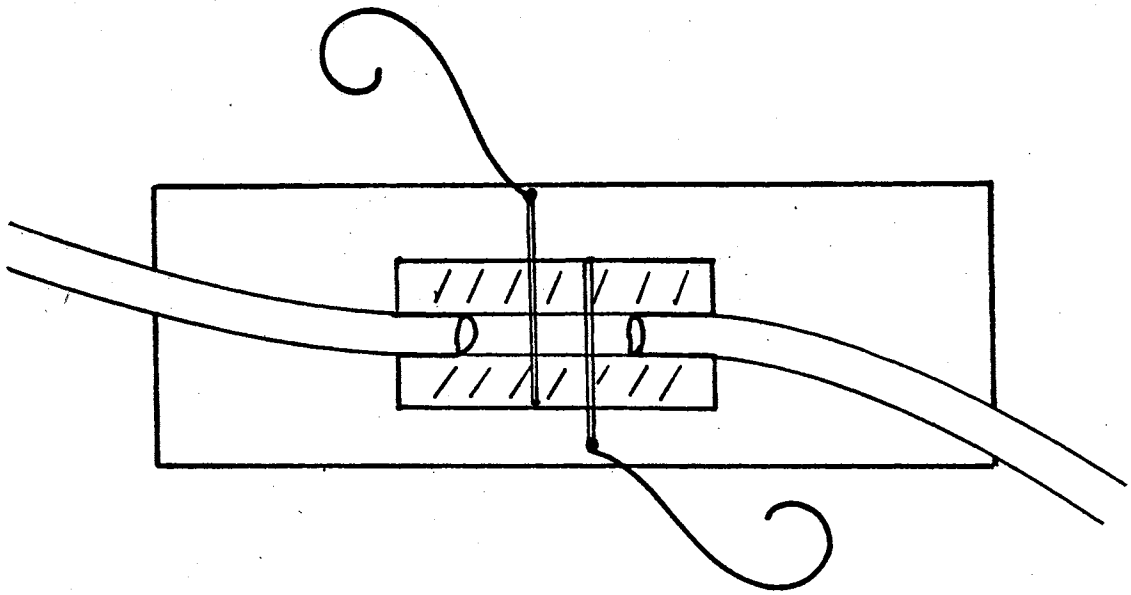

(A) TOP VIEW

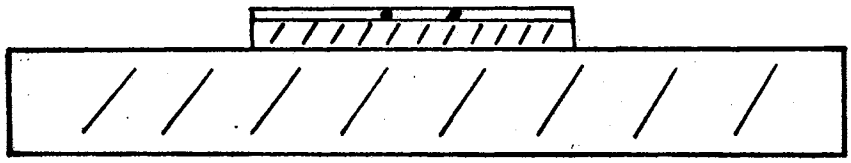

(B) SIDE VIEW

Figure 10. Detailed Views of the Assembled Continuous Dielectrophoresis Cell

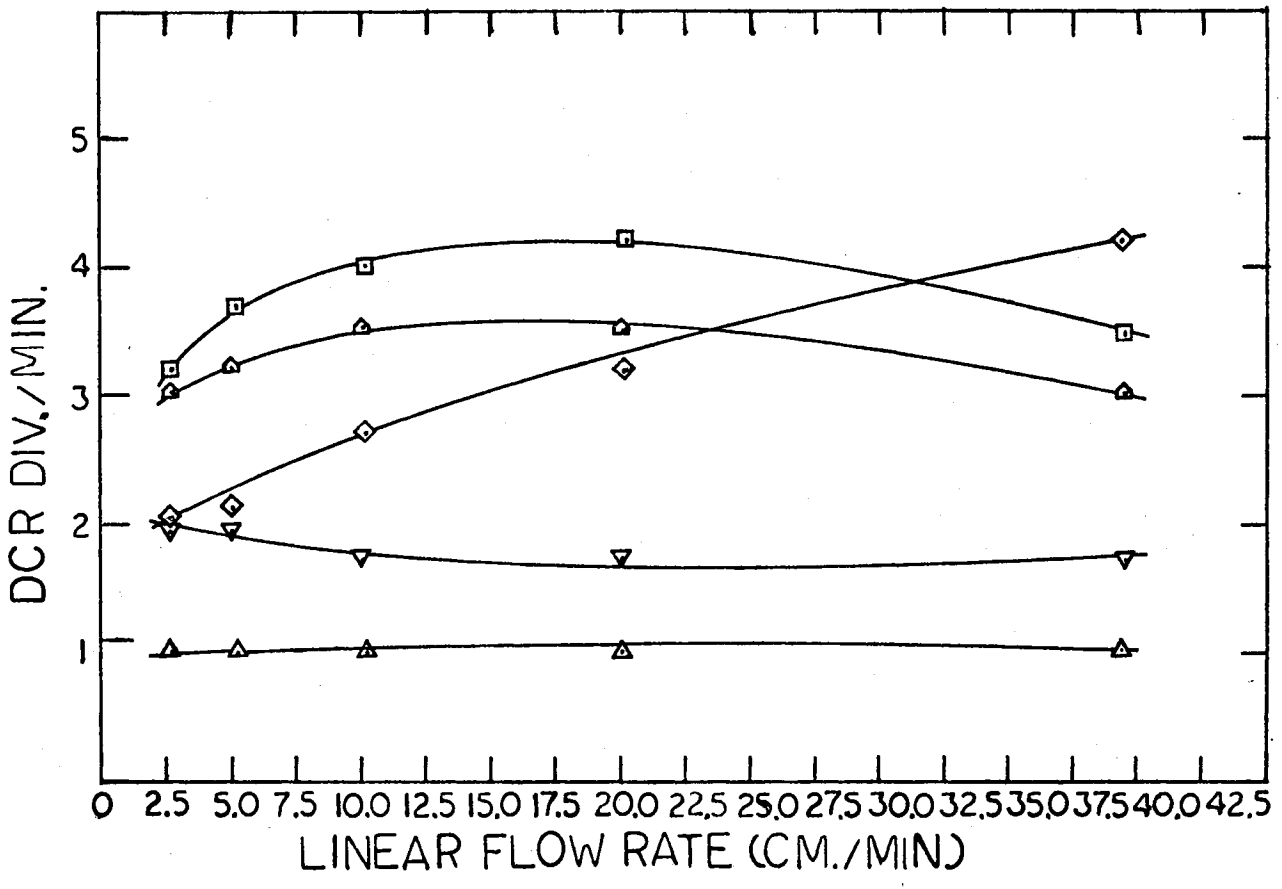

Figure 11. Dielectrophoretic Collection Rate (DCR) Versus Linear Flow Rate; 25 Micron Diameter Wire-Wire Electrodes, 20 Volts r.m.s., Collected at 1 Min., 210X; 0.3-0.5 Micron Particle Radius, pH = 9.0, $\rho = 0.184 \times 10^5$ ohm-cm, Optical Density = 0.28 at 550; (□) = 500 kHz, (⌂) = 100 kHz, (◇) = 2.55 MHz, (▽) = 2 kHz, (△) = 100 Hz

through the cell chamber and the field switched on for the chosen time of collection. After the yield was noted, the field was removed and the chamber washed with deionized water to dislodge any particles still clinging to the electrodes. The procedure was repeated until readings were obtained for all desired frequencies.

CHAPTER III

EXPERIMENTAL RESULTS AND DISCUSSION

Results

The Effect of pH

In Figure 12 are shown the collection rate versus frequency spectra for colloidal silica at solution pH's of approximately four, six and eight. Three features of the spectra are noted:

(1) At each pH there exist two distinct collection peaks, one in the 1-2 kHz range and the other in the 150-300 kHz range.

(2) In the central 5-30 kHz range the collection rate is not depressed to baseline.

(3) There is a general decrease in peak height with decrease in pH, the difference being most noticeable between pH's four and eight. The higher-frequency peak height, however, is greater at pH six than at pH eight. The peak also appears at a lower frequency than those of the pH four and pH eight spectra.

Particle Size

In Figure 13 are shown the collection spectra for two particle size ranges. The position of the high-frequency peak remains unaffected by change in particle size. The low-frequency peak, however, appears to be shifted to a higher frequency by a decrease in particle radius.

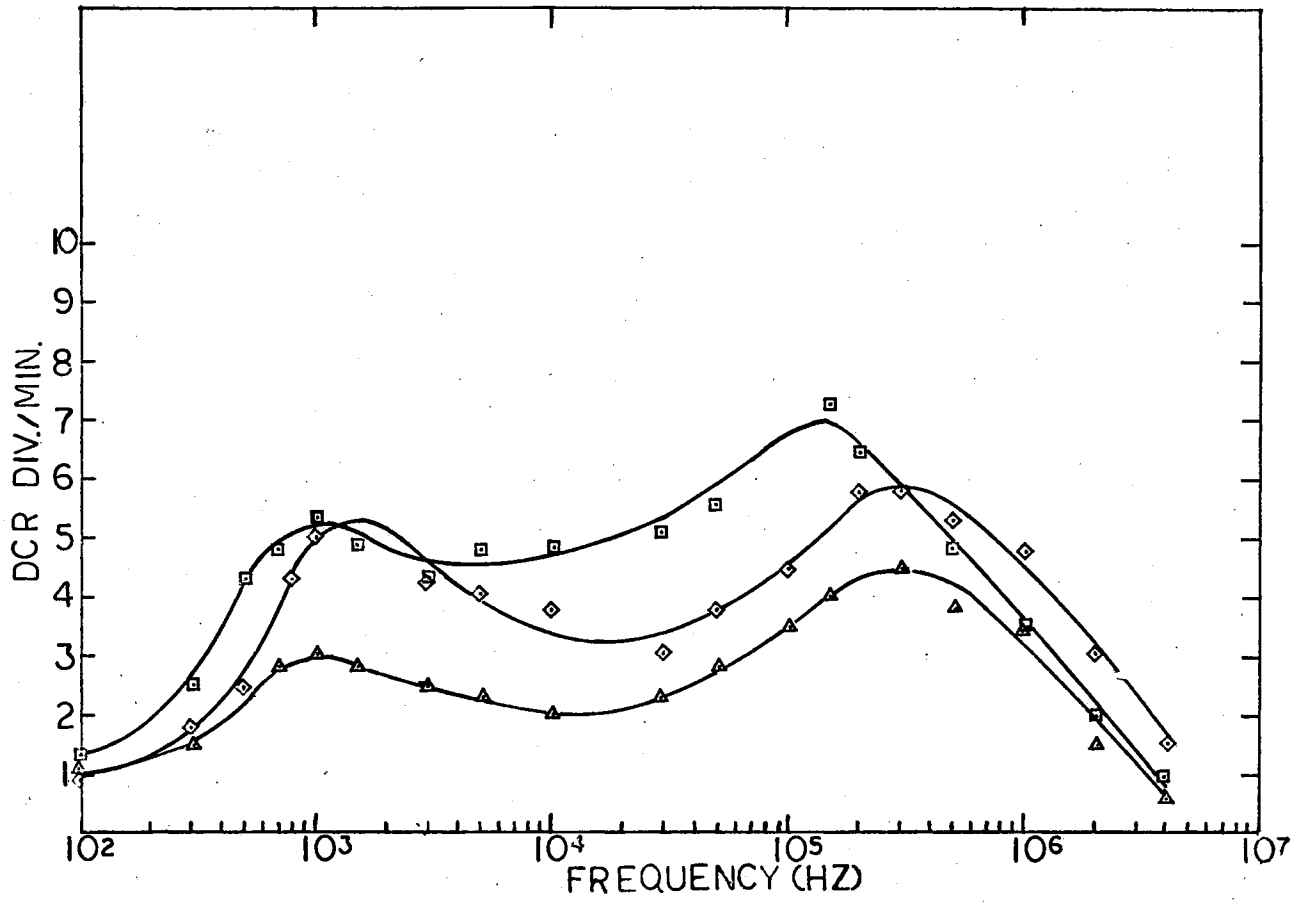

Figure 12. Effect of pH on the Dielectrophoretic Collection Rate of SiO_2; 25 Micron Diameter Wire-Wire Electrodes, 20 Volts r.m.s., Linear Flow Rate 10.2 cm/min, Collected in 1 Min., 210X, 0.3-0.5 Micron Particle Radius; (□) pH = 6.5, $\rho = 0.97 \times 10^5$ ohm-cm, Optical Density = 0.62 at 550, (◇) pH = 8.0, $\rho = 0.49 \times 10^5$ ohm-cm, Optical Density = 0.62 at 550, (△) pH = 4.4, $\rho = 0.50 \times 10^5$ ohm-cm, Optical Density = 0.64 at 550

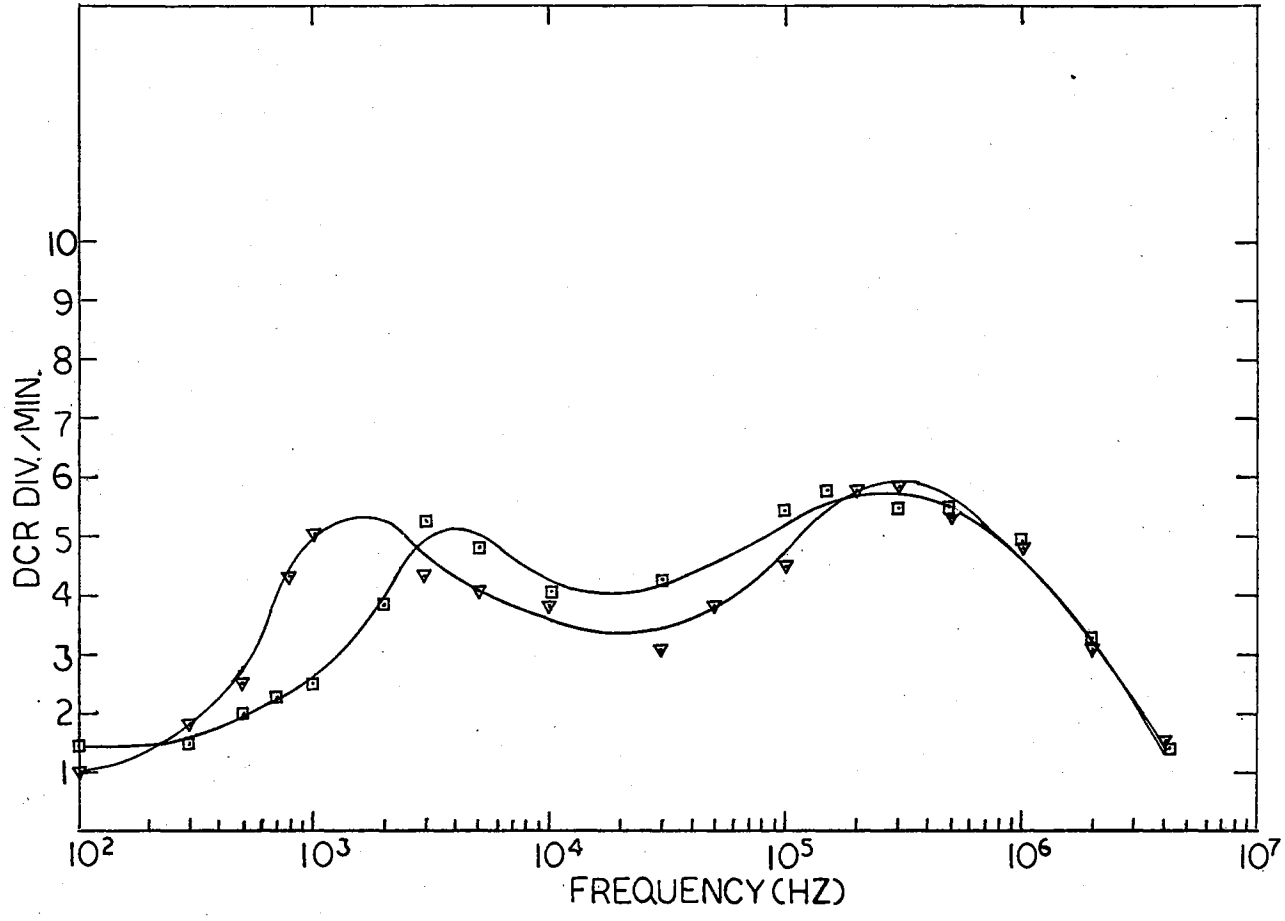

Figure 13. Effect of Particle Size on the Dielectrophoretic Collection Rate of SiO_2; 25 Micron Diameter Wire-Wire Electrodes, 20 Volts r.m.s., Linear Flow Rate 10.2 cm/min, 210X; (▽) = 0.3-0.5 Micron Particle Radius, pH = 8.0, ρ = 0.49 X 10^5 ohm-cm, Optical Density = 0.62 at 550, (□) = 0.2-0.3 Micron Particle Radius, pH = 8.3, ρ = 0.49 X 10^5 ohm-cm, Optical Density = 0.64 at 550

Ion Effects

Figure 14 illustrates the effect of cations upon the yield spectra of 0.3-0.5 micron SiO_2 at pH eight. The uppermost curve represents silica collection before the addition of electrolyte. The KNO_3, $Ca(NO_3)_2$ and $La(NO_3)_3$ solutions were each at a concentration of 0.05 millimolar. As the valence of the electrolyte cation increases, both high and low-frequency collection peaks are substantially depressed.

Optical Density Dependence

In Figure 15 are shown collection spectra for 0.3-0.5 micron SiO_2 at optical densities of 0.33, 0.60, and 0.90. As the optical density is decreased, the yield spectrum is lowered accordingly.

Discussion

The question now arises as to which, if any, of the mechanisms discussed are responsible for the increased yield in the 1-3 kHz and 200-300 kHz frequency ranges. The mechanisms chosen must possess relaxation times consistent with the observed frequency ranges, and further, must provide explanations for the variation of collection with experimental conditions. The theoretical quantity most easily compared with experiment is the mechanism relaxation time. The expression for the relaxation time of each of the four mechanisms will therefore be considered.

In the limit of zero volume fraction, the relaxation time for the volume interfacial polarization mechanism is given by:

$$\tau = \varepsilon_o \varepsilon_2 + 2\varepsilon_1/\sigma_2 + 2\sigma_1 \qquad (22)$$

and the corresponding characteristic frequency is $\frac{1}{2}\pi\tau$.

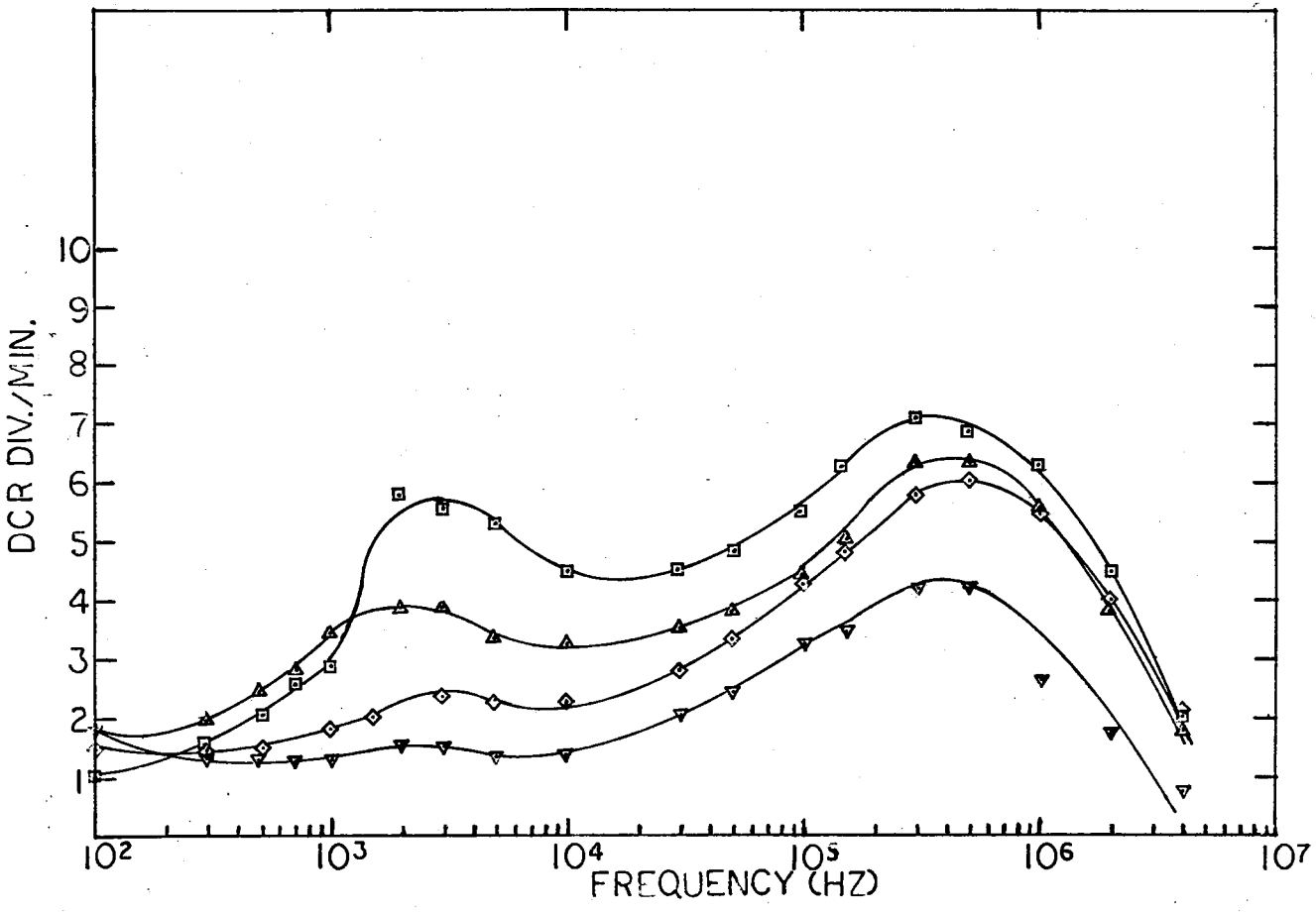

Figure 14. Effect of Cations on the Dielectrophoretic Collection Rate of SiO_2; 25 Micron Diameter Wire-Wire Electrodes, 20 Volts r.m.s., Linear Flow Rate 10.2 cm/min, Collected in 1 Min., 210X, 0.3-0.5 Micron Particle Radius; (□) pH = 7.8, ρ = 0.38 X 10^5 ohm-cm, Optical Density = 0.66 at 550, (△) = 0.05 mM KNO_3, pH = 7.8, ρ = 0.35 X 10^5 ohm-cm, Optical Density = 0.67 at 550, (◇) = 0.05 mM $Ca(NO_3)_2$, pH = 7.6, ρ = 0.31 X 10^5 ohm-cm, Optical Density = 0.64 at 550, (▽) =0.05 mM $La(NO_3)_3$, pH-7.6, ρ =0.31 X 10^5 ohm-cm, Opt. Dens.=0.67 at 550

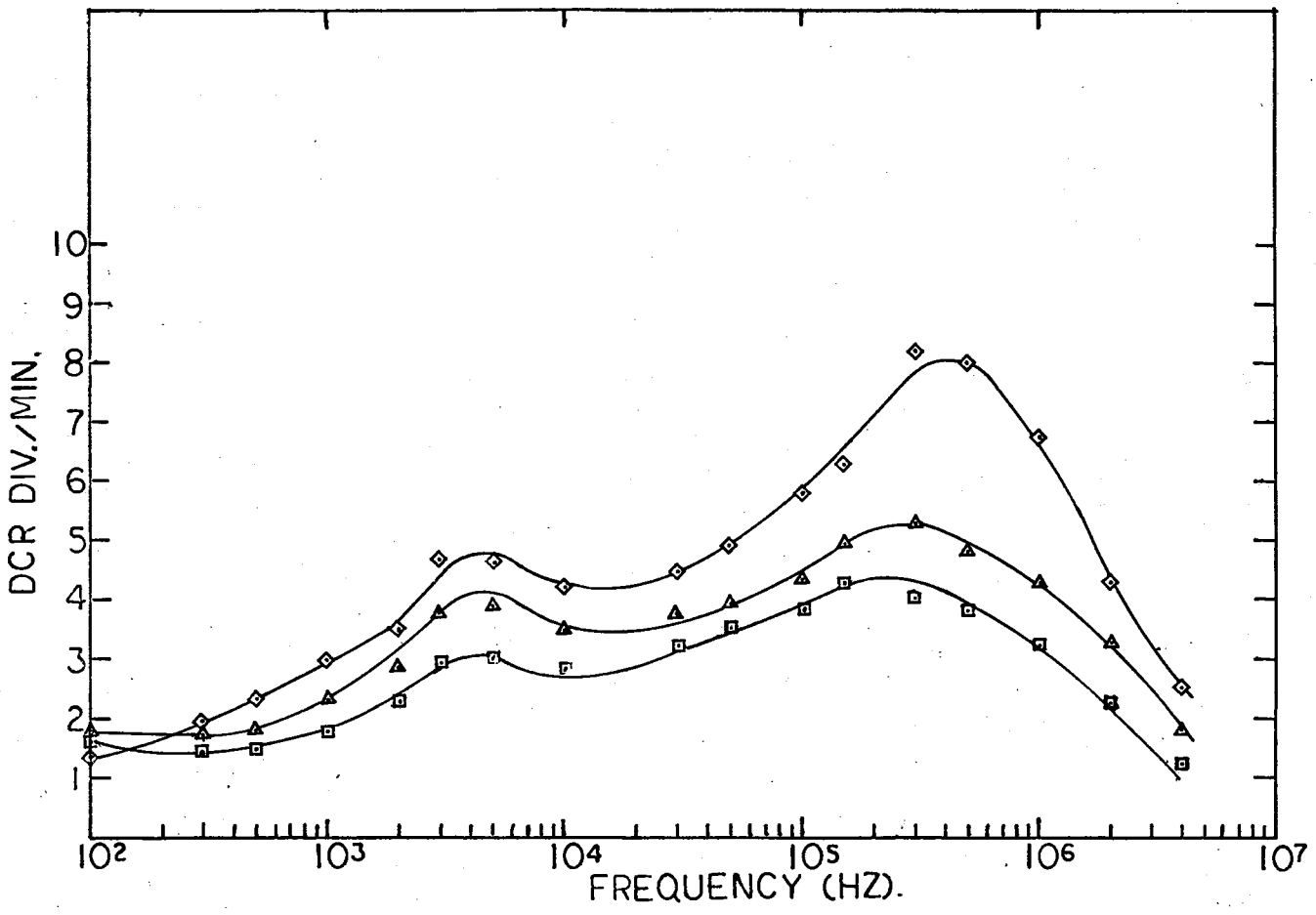

Figure 15. Effect of Optical Density on the Dielectrophoretic Collection Rate of SiO_2; 25 Micron Diameter Wire-Wire Electrodes, 20 Volts r.m.s., Linear Flow Rate 10.2 cm/min, Collected in 1 Min., 210X, 0.3-0.5 Micron Particle Radius; (◇) Optical Density=0.9 at 550, pH=8.2, $\rho = 0.40 \times 10^5$ ohm-cm, (△) Optical Density=0.60 at 550, pH=8.2, $\rho = 0.43 \times 10^5$ ohm-cm, (□)=Optical Density=0.33 at 550, pH=8.4, $\rho = 0.46 \times 10^5$ ohm-cm

Employing values of: $\varepsilon_1 = 78$ $\varepsilon_2 \simeq 4$ (2)

$$\sigma_1 = 2 \times 10^{-5} \text{ mho-cm}^{-1} \qquad \sigma_2 = 10^{-18} \text{ mho-cm} \qquad (24)$$

$$\varepsilon_o = 8.85 \times 10^{-14} \text{ Coulomb/Volt-cm}$$

the characteristic frequency is approximately 400 kHz. Hence, on the basis of relaxation time alone, the volume interfacial polarization mechanism must be considered as an explanation for the high-frequency collection peak.

The expression for the relaxation time of the modified interfacial polarization mechanism is identical to that for the volume mechanism except for the term $2\lambda_s/a$ appearing in the denominator:

$$\tau = \varepsilon_o(\varepsilon_2+2\varepsilon_1) \; / \; \sigma_2 + 2\lambda_s/a + 2\sigma_1 \qquad (23)$$

It is the surface conductance, λ_s, that is of primary interest. The approximation $\lambda_s = e_o^2 \sigma_o u$ is made and the factors to be determined are the surface charge density and the counterion mobility. For colloidal silica at a pH of eight and under conditions similar to those of this study, Bolt (25) has found the surface charge density to be in the order of 10^{12} per square centimeter. Sodium, with a mechanical mobility of 3.4×10^{15} cm^2/Coulomb-volt-second, is assumed as the counterion. The surface conductance is then in the order of 10^{-10} mho and the calculated characteristic frequency is in the 400-500 kHz range. The modified interfacial polarization mechanism must therefore be considered as a contributor to the high-frequency peak.

The relaxation time for the bound-counterion polarization mechanism is given by: $\tau = a^2/2u_b kT$ (12)

where $u_b = u_o e^{-\alpha/kT}$ and alpha is the potential barrier height. Assuming sodium as the counterion, along with a potential barrier height of 1 kcal/mole (1.6 kT/mole) and a particle radius of 0.4 micron,

the characteristic frequency is in the order of 1 kHz and the bound-counterion mechanism may contribute to the low-frequency collection peak.

If distortion of the diffuse portion of the double layer is taken into account, the bound-ion mobility of equation 12 is replaced by that of the free ion: $\tau_{diffuse} = a^2/2u_okT$ (17)
The calculated frequency is then 2-3 kHz and the contribution of the diffuse atmosphere distortion polarization to the low-frequency peak must be considered.

It would appear that, on the basis of relaxation times alone, the high-frequency peak may be explained in terms of volume and modified interfacial polarization, while the low-frequency peak may be considered to arise from bound-ion and diffuse atmosphere distortion polarization. The final choice of mechanisms, however, must be based upon comparison of all aspects of the proposed theories with experimental results. Just as the relaxation times of the mechanisms may be related to the frequencies at which collection peaks occur, the dielectric increments for the mechanisms may be related, through the dipole moment per particle, to the observed peak heights. Any circumstance which serves to decrease the suspension dielectric increment should produce a corresponding decrease in the particle dielectrophoretic collection rate. The dielectric increment thus provides a second criterion by which the suggested mechanisms may be evaluated.

The most obvious decrease in peak height is that brought about by the addition of electrolytes. Both high and low-frequency peak collection is reduced as the valence of the electrolyte counter-ion increases. The dielectric increment expressions for the mechanisms chosen should accurately reflect the observed decrease in peak height.

The dielectric increments for the mechanisms suggested as responsible for the low-frequency peak are given by:

$$\Delta\varepsilon_{\text{bound ion}} = 9/4\ p/(1+p/2)^2\ \frac{e_o^2 a \sigma_o}{\varepsilon_o kT} \tag{15}$$

$$\Delta\varepsilon_{\text{diffuse}} = 9/2\ p(3m\ \exp(e\zeta/kT)+\exp(e\Psi^{\beta}/kT))^2 \tag{18}$$

As electrolyte is added to the colloidal suspension, double layer theory predicts that the surface charge density, as well as the potentials at the outer Helmholtz plane and the hydrodynamic plane of shear, may be lowered. Therefore, both the bound-counterion mechanism (through σ_o) and the diffuse atmosphere mechanism (through ζ and Ψ^{β}) are in accordance with experimental observation.

In the limit of zero volume fraction, the dielectric increments for the mechanisms suggested as responsible for the high-frequency peak are given by:

$$\Delta\varepsilon_{\text{volume}} = 9p\ (\varepsilon_1\sigma_2-\varepsilon_2\sigma_1)^2/(\varepsilon_2+2\varepsilon_1)(\sigma_2+2\sigma_1)^2 \tag{24}$$

$$\Delta\varepsilon_{\text{modified}} = \frac{9p(\varepsilon_1(\sigma_2+2\lambda_s/a)-\varepsilon_2\sigma_1)^2}{(\varepsilon_2+2\varepsilon_1)\ (\sigma_2+2\lambda_s/a+2\sigma_1)^2} \tag{25}$$

Under conditions of constant volume fraction, only one parameter in equation 24, σ_1, may vary. Any reduction of suspension dielectric increment upon addition of electrolyte must therefore be attributed to variation in medium conductivity. It may be seen from Figure 14 that the solution resistivity remains essentially constant as the cation valence is increased. The variation in σ_1 is thus far too small to account for the large decrease in peak yield and the volume interfacial polarization mechanism must be eliminated as a possible contributor to the high-frequency peak.

The dielectric increment expression for the modified interfacial polarization mechanism contains the surface charge density σ_o in the

term approximating the surface conductance λ_s. Inspection of the equation reveals that a decrease in surface density will lead to a decrease in dielectric increment. Hence, if the addition of electrolyte is assumed to reduce σ_o, the dielectric increment expression for the modified interfacial polarization mechanism faithfully reflects the observed decrease in yield.

In summary, then, upon consideration of both relaxation time and dielectric increment, the bound-counterion and diffuse atmosphere mechanisms may be associated with the low-frequency (1-3 kHz) collection peak while the modified interfacial polarization mechanism may be associated with the high-frequency (200-300 kHz) collection peak.

Comparison With Experiment

Once specific mechanisms have been conditionally assigned, it becomes necessary to review the experimental results in greater detail. Comparison of observed dielectrophoretic collection behaviour with that predicted by theory provides further information concerning the appropriateness of the mechanisms chosen.

The Effect of pH

Since the charging of the silica surface has been attributed to the dissociation of silanol groups, the surface charge density and subsequent development of the double layer should be highly dependent upon solution pH. The magnitude of the surface charge density is expected to be appreciable at pH eight, slightly less at pH six, and minimal at pH four as the isoelectric point is approached.

The low-frequency peak, associated with the theories of double layer distortion polarization, roughly approximates the predicted trend. The peak height is not noticeably depressed as the pH is lowered from eight to six, but is considerably reduced around pH four. Thus, the behaviour predicted from the dielectric increment expressions for the assigned mechanisms is in qualitative agreement with experiment.

The high-frequency peak, associated with the modified interfacial polarization mechanism, appears to exhibit marked deviation from theory. The dielectric increment expression of Equation 25 indicates that a decrease in surface charge density should produce a corresponding decrease in dielectrophoretic collection rate. A comparison of the spectra for pH's four and eight confirms this assumption, but as previously noted, the high-frequency peak at pH six is higher and appears to the left of the other. Further examination of Equations 25 and 23 reveals a possible explanation. The relaxation time for the interfacial polarization mechanism is inversely proportional to the conductivity of the suspending medium. Previous studies (20) have found that as the conductivity of the medium is decreased, the characteristic peak frequency is shifted to lower values. The solution conductivity for the spectra obtained at pH's four and eight is approximately 2×10^{-5} mho-cm^{-1}, while the conductivity for the spectrum at pH six is 1.03×10^{-5} mho-cm^{-1}. The high-frequency peak for the latter spectrum should therefore appear at a lower frequency. The variation in medium conductivity may also explain the relative peak heights of the pH eight and pH six spectra. As the conductivity of the medium is decreased, the dielectric increment for the modified interfacial polarization mechanisms is increased. Thus, it may also be argued that lower solution

conductivity at pH six results in an increase in high-frequency peak height. These two arguments were tested by obtaining another pH six dielectrophoretic collection rate spectrum (Figure 16), this time with solution conductivity adjusted by $NaNO_3$ to a value closely approximating those of the pH four and eight spectra. The high-frequency peak then shifted to a higher frequency value, comparable to those of the other pH spectra. Unfortunately, since the spectrum was obtained with a different dielectrophoresis cell, the absolute peak heights at pH's four, six, and eight cannot be compared. However, the peak shift does indicate that it was the solution conductivity, σ_1, which was responsible for the unexpected behaviour at the original pH six spectrum.

Particle Size

The relaxation time for the modified interfacial polarization mechanism is largely independent of size for spherical particles. The relaxation times for the bound-ion and diffuse atmosphere mechanisms, however, are directly proportional to the square of the particle radius. Therefore, if two spectra are obtained under conditions similar except for particle size, the position of the high-frequency peak should remain unchanged while that of the low-frequency peak should be shifted in the appropriate direction. These are precisely the results illustrated in Figure 13. A decrease in particle size from 0.3-0.5 micron to 0.2-0.3 micron leaves the high-frequency peak centered around 300 kHz while shifting the low-frequency peak from 1.5 kHz to 4 kHz. Since the characteristic frequency f for the double layer distortion mechanisms is given by: $f = ukT/\pi a^2$, a decrease in particle radius has the effect of shifting the low-frequency peak to higher frequency values.

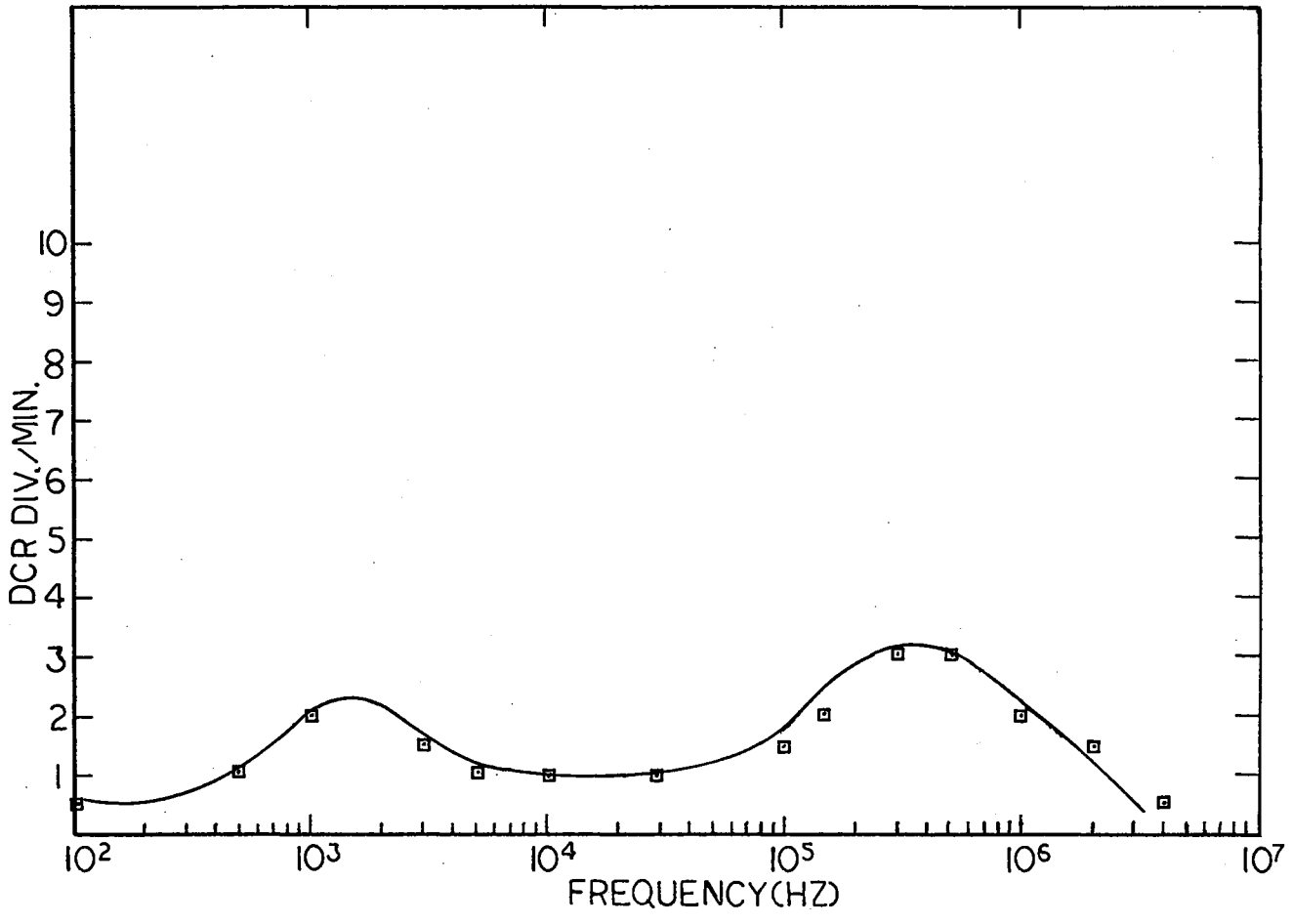

Figure 16. Repeat of pH Six Dielectrophoretic Collection Rate Spectrum; 25 Micron Diameter Wire-Wire Electrodes, 20 Volts r.m.s., Linear Flow Rate 10.2 cm/min, Collected in 1 Min., 210X, 0.3-0.5 Micron Particle Radius; pH = 6.1, $\rho = 0.45 \times 10^5$ ohm-cm, Optical Density = 0.58 at 550

Ion Effects

As noted in the earlier discussion of dielectric increments, the addition of electrolyte to a colloidal suspension may reduce the surface charge density, the potential at the outer Helmholtz plane, and the electrokinetic zeta potential. An increase in the valence of the electrolyte counterion enhances the reduction. Figure 14 illustrates the depression of yield peaks for both high and low frequency regions. Interpretation of the results is complicated by slight flocculation of the colloidal silica in the presence of the triply-charged lanthanum ion. The lanthanum collection spectrum may be more than proportionately depressed because of sedimentation of large aggregates of silica particles. Nonetheless, it may be seen that the addition of electrolyte does decrease the dielectrophoretic collection rate in the manner predicted by the dielectric increment expressions for each of the chosen mechanisms.

Mutual Dielectrophoresis

Since the surface double layer figures prominently in each of the mechanisms chosen, some correlation between high and low-frequency peak behaviour is expected. In particular, a qualitative comparison of peak height ratios under conditions of varying pH or ionic valence should reflect relative changes in mechanism dielectric increment. A comparison of this sort may be prevented, however, by the effect of mutual dielectrophoresis (26).

The phenomenon of mutual dielectrophoresis arises from the distortion of an applied electric field by the polarizable particles of a colloidal suspension. The distortion results in the presence of a

nonuniform field in the vicinity of each particle. The particles are then mutually attracted by the regions of higher field intensity, forming aggregates ranging in composition from bunch-like clumps to long pearl-chains directed along the axes of the applied field. The association of suspended particles may increase the dielectrophoretic collection rate beyond that predicted by single-particle calculations.

It has been observed in this and other studies (20) that the nature of low-frequency collection is qualitatively different from that at higher frequencies. Particles tend to collect in clumps at low frequencies and in long chains as the frequency is increased. It has also been suggested that, in addition to the frequency dependence, pearl-chain formation exhibits a dependence upon particle concentration (27). It is therefore possible that the yield, measured as the linear growth of collected particles from the surface of the electrode, reflects not only the absolute dielectrophoretic force but also the magnitude and form of mutual dielectrophoresis. Before a comparison of low and high-frequency peak heights can be made, it is necessary to attempt an evaluation of the relative contribution of mutual dielectrophoresis under the conditions of frequency and particle concentration employed.

In Figure 17 are represented the values of high and low-frequency peak collection as a function of optical density. Up to optical densities of around 0.6, the slopes of the two curves are approximately equal. At higher optical densities, however, the high-frequency curve undergoes a marked increase in slope. This result suggests that at high particle concentrations, pearl-chain formation is disproportionately increasing the high-frequency collection. The optical densities

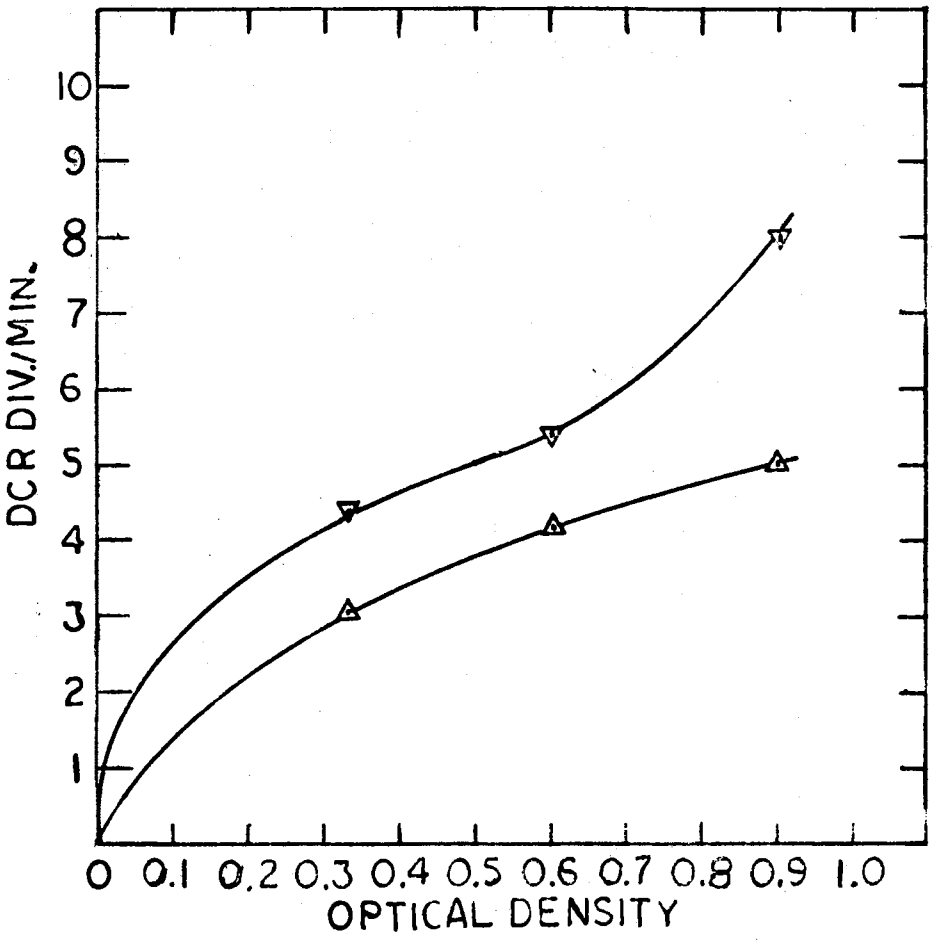

Figure 17. Dielectrophoretic Collection Rate Versus Optical Density for High and Low-Frequency Peaks; 25 Micron Diameter Wire-Wire Electrodes, 20 Volts r.m.s., Linear Flow Rate 10.2 cm/min, Collected in 1 Min., 210X, 0.3-0.5 Micron Particle Radius; (▽) = High-Frequency Peak Collection Rate, (△) = Low-Frequency Peak Collection Rate

employed in this study were in the neighborhood of six-tenths. It appears, then, that qualitative comparison of the low and high-frequency collection peaks is not precluded by the contribution of mutual dielectrophoresis.

Comparison of Low and High-Frequency Peaks

Figure 14 indicates that the addition of electrolyte affects the low-frequency peak to a greater extent than the high-frequency peak. The ratio of high to low-frequency peak heights is roughly 1.2 in the absence of electrolyte, 1.8 for K^+, 2.4 for Ca^{2+}, and 2.7 for La^{3+}. Since the precise reduction in surface charge density produced by a given concentration of electrolyte cation is not known, a quantitative comparison of the relative change in dielectric increment for the low and high-frequency mechanisms as a function of cation valence cannot be attempted. However, further studies may allow correlation of the relative changes in dielectric increment with the observed increase in high to low-frequency peak height ratio.

The Possibility of a Third Peak

It has been noted that in the central 5-30 kHz region of the frequency spectra for colloidal silica, the collection is not depressed to baseline. This suggests either an appreciable overlap of high and low-frequency peak tails or the presence of a third peak, obscured by the positions of the other two. According to the expressions for the relaxation times of the low-frequency mechanisms, an increase in particle radius should shift the low-frequency peak to the left. If the peak is shifted far enough, the existence of any central peak may be ascertained.

In Figure 18 the collection rate versus frequency spectrum for 0.5-0.7 micron SiO_2 is shown. A questionable peak is observed at very low (600-700 Hz) frequencies and the high-frequency peak is centered in the 200-300 kHz range. In addition, there is an apparent peak shoulder in the central 2-30 kHz region. The possibility of a third peak must therefore be considered. The origin of such a peak may only be speculated upon. Collection in the central region appears to be decreased by the same conditions of pH and ionic valence that depress the two rate peaks. Thus, an explanation for the enhanced collection in the 5-30 kHz range may also involve the surface double layer.

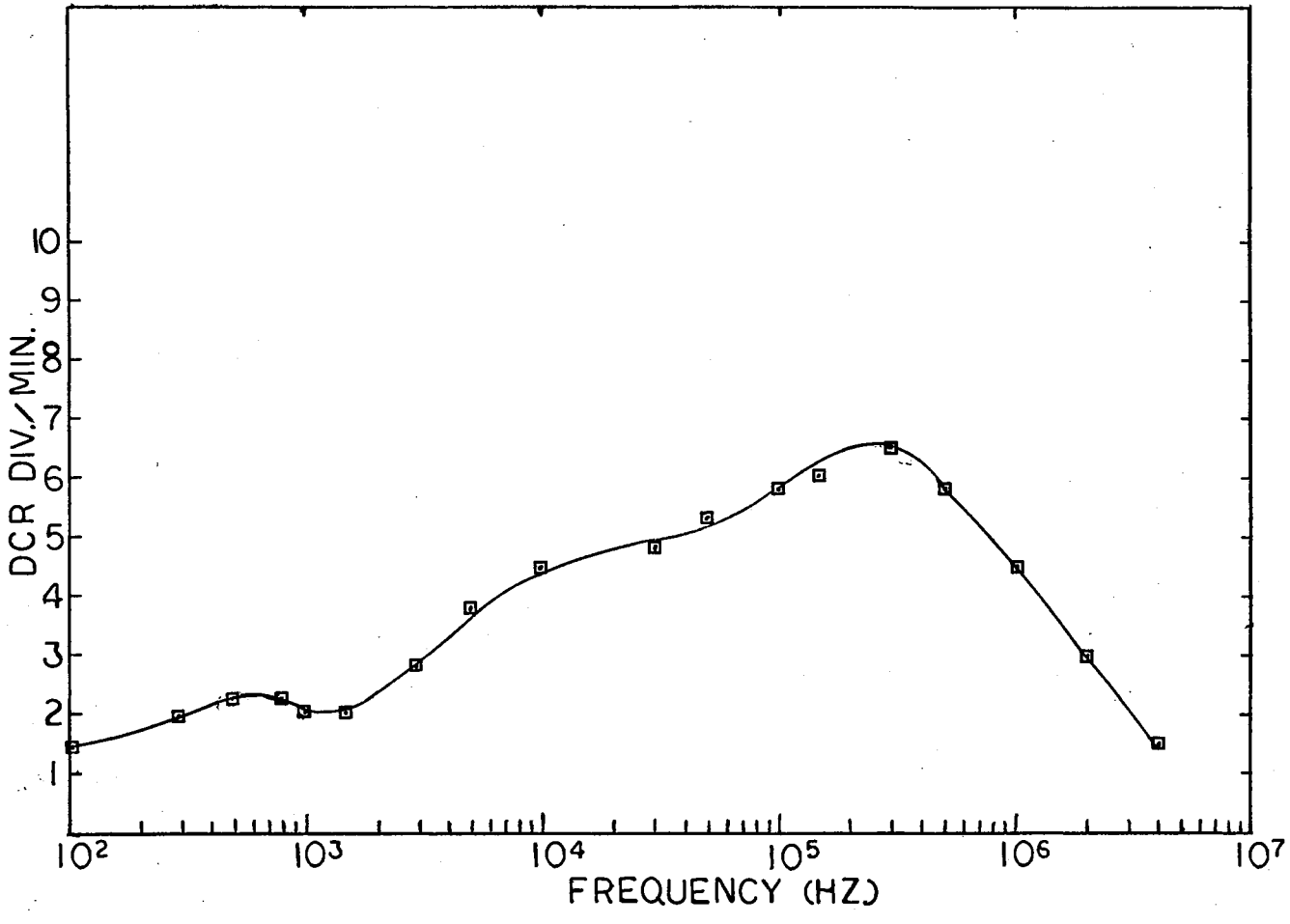

Figure 18. Dielectrophoretic Collection Rate Versus Frequency Spectrum for 0.5-0.7 Micron SiO_2; 25 Micron Diameter Wire-Wire Electrodes, 20 Volts, r.m.s., Linear Flow Rate 10.2 cm/min, Collected in 1 Min., 210X; pH = 8.2, $\rho = 0.45 \times 10^5$ ohm-cm, Optical Density = 0.64 at 550

CHAPTER IV

SUMMARY AND SUGGESTIONS FOR FUTURE STUDY

Two distinct dielectrophoretic collection rate peaks have been observed in the rate versus frequency spectra of colloidal silica. The low-frequency (1-3 kHz) peak has been associated with both the bound-counterion and diffuse atmosphere distortion polarization mechanisms. The high-frequency (200-300 kHz) peak has been related to the modified interfacial polarization mechanism.

Because of the particle-size dependence of the low-frequency mechanisms, future dielectrophoretic studies should be carried out with monodisperse suspensions of well-defined particle radius. The concentration and frequency dependence of mutual dielectrophoresis should be further investigated if comparison of high and low-frequency peak heights is desired.

The determining factor in the success of future studies, however, is the use of single-cell dielectrophoresis. The technique, described in detail by Chen (28), involves the application of a non-uniform field to individual colloidal particles. The method is thermodynamic in nature rather than kinetic, and thus eliminates several problematical features inherent in the many-particle system:

(1) At the low (~ 1 volt) electric field strengths utilized, the thermal gradient and charge injection effects giving rise to interelectrode circulation and pulsing may be reduced.

(2) Since the quantity of interest is the particle release voltage, rather than the yield, the complication of mutual dielectrophoresis is removed.

(3) The apparent discrepancy between yield magnitude and collection rate (saturation effect) is avoided.

Moreover, the excess permittivity measured by the single-cell technique is directly concerned with the effective polarizability of the particle itself, and may be readily related to volume and surface properties. The technique of single-cell dielectrophoresis may thus prove an ideal method for further investigations of the surface double layer.

BIBLIOGRAPHY

1. Anderson, J. C., Dielectrics, Reinhold Publishing Corporation, New York (1964).

2. Schwan, H. P., G. Schwarz, J. Maczuk and H. Pauly, J. Phys. Chem., 66, 2626 (1962).

3. Mysels, K. J., Introduction to Colloid Chemistry, Interscience Publishers, Inc., New York (1959).

4. Carman, P. C., Trans. Faraday Soc., 36, 964 (1940).

5. Iler, R. K., Surface and Colloid Science, 6, 1 (1970).

6. Allen, L. K., and E. Matijevic, J. Colloid Inter. Sci., 33, 420 (1970).

7. Iler, R. K., The Colloid Chemistry of Silica and Silicates, Cornell University Press, Ithaca (1955).

8. O'Konski, C. T., J. Phys. Chem., 64, 605 (1960).

9. Sieglaff, C. L., and J. Maxur, J. Colloid Sci., 15, 437 (1960).

10. Schwarz, G., J. Phys. Chem., 66, 2636 (1962).

11. Shilov, V. N., and S. S. Duhkin, Colloid J., 32, 245 (1970).

12. Duhkin, S. S., Surface and Colloid Science, 3, 83 (1971).

13. Mandel, M., Mod. Phys., 4, 489 (1961).

14. Debye, P., Polar Molecules, Chem. Catalog Co., Inc., New York (1929).

15. Kirkwood, J. G., and J. B. Shumaker, Proc. Natn. Accd. Sci., U.S.A., 38, 855 (1952).

16. Jacobsen, B., J. Am. Chem. Soc., 77, 2917 (1955).

17. Pohl, H. A., J. Appl. Phys., 22, 869 (1951).

18. Pohl, H. A., J. Appl. Phys., 29, 1182 (1958).

19. Crane, J. S., "The Dielectrophoresis of Cells" (unpub. Ph.D. thesis, Oklahoma State University, 1967).

20. Chen, C., "On the Nature and Origins of Biological Dielectrophoresis" (unpub. Ph.D. thesis, Oklahoma State University, 1973).

21. Shilov, N. N., and Y. F. Deinega, Colloid J., 31, 731 (1969).

22. Pohl, H. A., and J. S. Crane, Biophys. J., 11, 711 (1971).

23. Sedwick, T. O., J. Electrochem. Soc., 118, 349 (1971).

24. Handbook of Chemistry and Physics, 49th ed., Cleveland (1968).

25. Bolt, G. H., J. Phys. Chem., 61, 1166 (1957).

26. Pohl, H. A., "Nonuniform Field Effects: Dielectrophoresis," Electrostatics and Its Applications, ed. A. D. Moore, Wiley-Interscience, New York (1973).

27. Vorob'eva, T. A., I. N. Vlodavets, and P. I. Zubar, Colloid J., 31, 533 (1969).

28. Chen, C., and H. A. Pohl, Trans. New York Acad. Sci., in press (1974).

VITA

Cynthia Gail Scrimager

Candidate for the Degree of

Master of Science

Thesis: DIELECTROPHORESIS OF INORGANIC COLLOIDAL SUSPENSIONS

Major Field: Chemistry

Biographical:

Personal Data: Born in Chickasha, Oklahoma, August 10, 1950, the daughter of Richard and Colene Walters Scrimager.

Education: Graduated from Chickasha High School, Chickasha, Oklahoma, in 1967; received the Bachelor of Science degree from the University of California at Berkely in June, 1973, with a major in chemistry; completed the requirements for the Master of Science degree at Oklahoma State University in December, 1974.